Chapter 2

Physics of Josephson Junctions:

The Zero Voltage State

2.1 Basic properties of lumped Josephson junctions

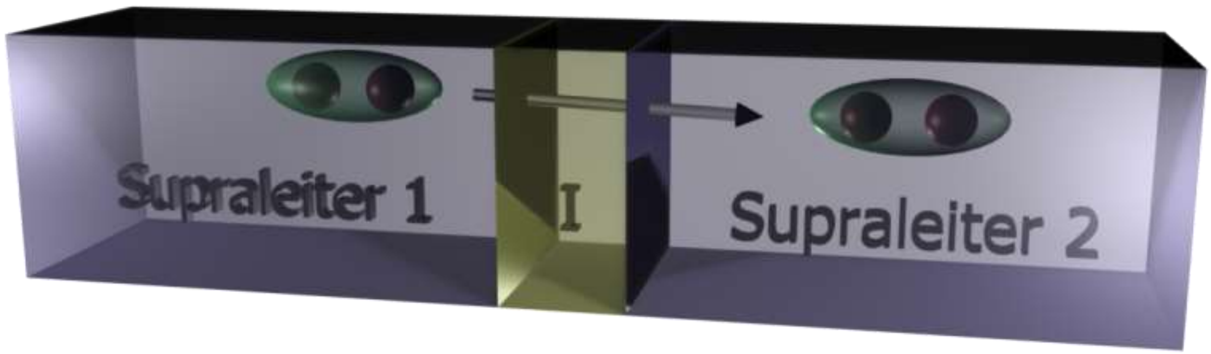

Small spatial dimensions:

→ Gauge invariant phase diff. & current density are uniform

→ variations of supercurrent density on length scale larger than λ_{L}

$$\lambda_{\mathrm{L}} = \sqrt{\frac{m_{\mathrm{s}}}{\mu_0 n_{\mathrm{s}} q_{\mathrm{s}}^2}} \approx 10^{-2}\ \mu\mathrm{m} - 1\ \mu\mathrm{m}$$

Josephson junction: n_{s} strongly reduced:

$\lambda_{\mathrm{L}} \rightarrow \lambda_{\mathrm{J}} \approx 10\ \mu\mathrm{m} - 100\ \mu\mathrm{m}$ (Josephson penetration depth)

2.1.1 The Lumped Josephson Junction

Spatially homogeneous supercurrent density and phase difference → Lumped element JJ

$$I_s = \int_S \mathbf{J}_s \cdot d\mathbf{s}$$ Region of integration is junction area S

Current-phase relation $$I_s(t) = I_c \sin\varphi(t)$$

Gauge invariant phase difference $$\varphi(t) = \theta_2(t) - \theta_1(t) - \frac{2\pi}{\Phi_0}\int_1^2 \mathbf{A}(\mathbf{r},t)\cdot d\mathbf{l}$$

2-nd Josephson relation $$\frac{\partial\varphi}{\partial t} = \frac{2\pi}{\Phi_0}\int_1^2 \mathbf{E}(\mathbf{r},t)\cdot d\mathbf{l} \quad \Rightarrow \quad \frac{d\varphi}{dt} = \frac{2\pi}{\Phi_0} V$$

Uniform phase difference → Total derivative

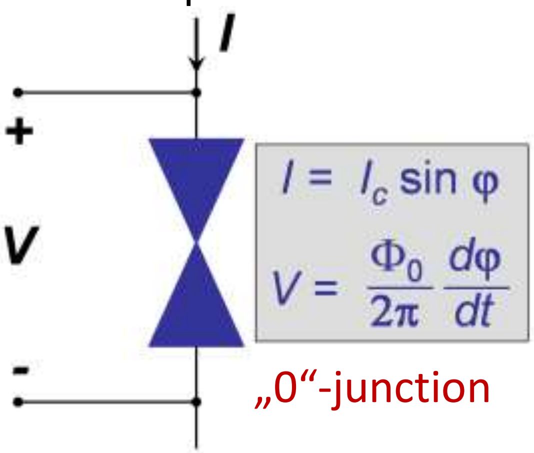

„0"-junction

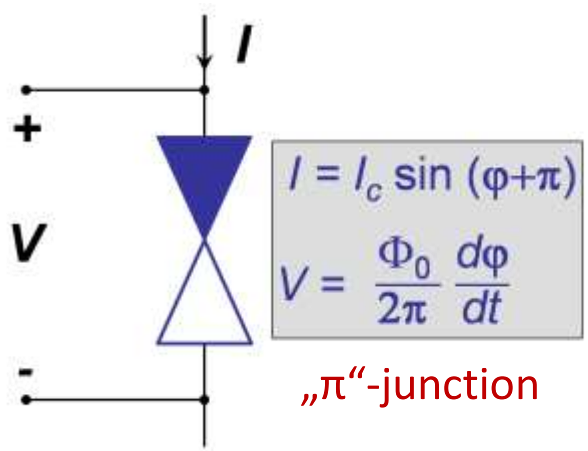

„π"-junction

outdated symbols (rarely ever used)

up-to-date symbols
for Josephson junctions
(both "0" and "π")

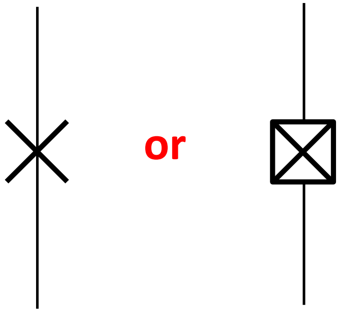

2.1.2 The Josephson coupling energy

Finite energy stored in JJ: overlap of macroscopic wave functions → Binding energy

Initial current & phase difference → Zero

Increase junction current from zero to a finite value

→ Phase difference has to change

→ 2-nd Josephson relation: finite-voltage state in a junction

→ External source has to supply energy (to accelerate the superelectrons)

→ Stored kinetic energy of moving superelectrons

→ Integral of the power $= I_s V$ (voltage during current increase)

$$E_J = \int_0^{t_0} I_s V \, dt = \int_0^{t_0} (I_c \sin\tilde{\varphi}) \left(\frac{\Phi_0}{2\pi}\frac{d\tilde{\varphi}}{dt}\right) dt \overset{\substack{\tilde{\varphi}(0)=0 \\ \tilde{\varphi}(t_0)=\varphi}}{=} \frac{\Phi_0 I_c}{2\pi}\int_0^{\varphi} \sin\tilde{\varphi}\, d\tilde{\varphi}$$

Integration →
$$\boxed{E_J = \frac{\Phi_0 I_c}{2\pi}(1-\cos\varphi) = \underbrace{E_{J0}(1-\cos\varphi)}_{\text{Josephson coupling energy}}}$$

2.1.2 The Josephson coupling energy

Josephson coupling energy

$$E_\mathrm{J} = \frac{\Phi_0 I_\mathrm{c}}{2\pi}(1-\cos\varphi) = E_\mathrm{J0}(1-\cos\varphi)$$

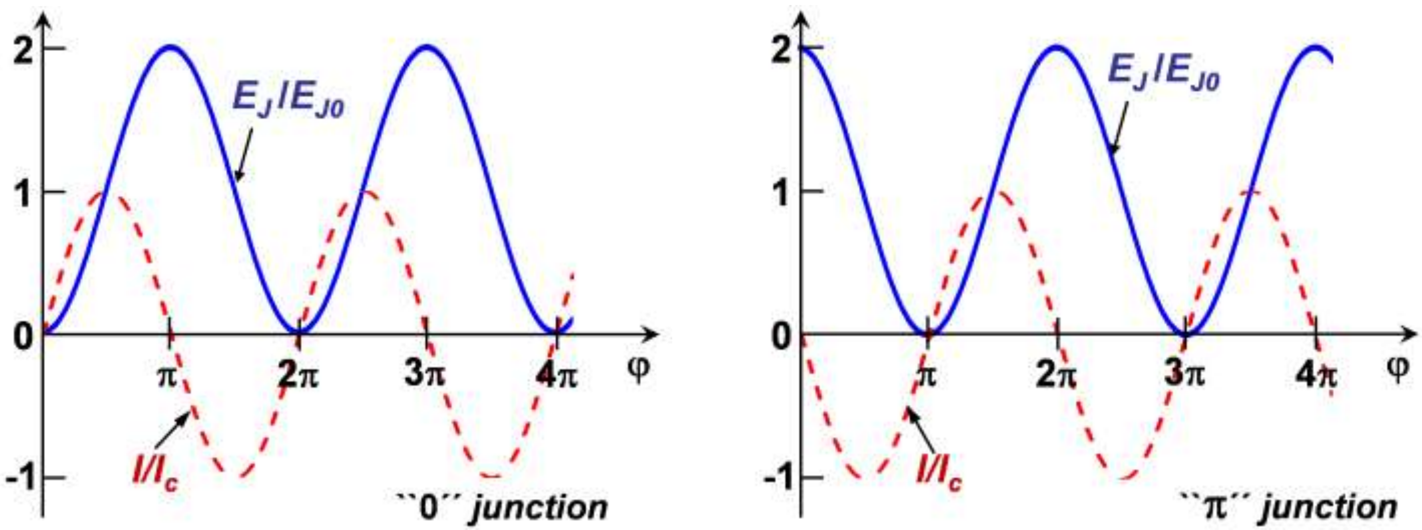

Order of magnitude

→ Traditional applications → $I_\mathrm{c} \approx 1\ \mathrm{mA}$ → $E_\mathrm{J0} \approx 3\times 10^{-19}\ \mathrm{J} \approx k_\mathrm{B}\times 20000\ \mathrm{K}$

→ Quantum circuits: $I_\mathrm{c} \approx 1\ \mu\mathrm{A}$ → $E_\mathrm{J0} \approx 3\times 10^{-22}\ \mathrm{J} \approx k_\mathrm{B}\times 20\ \mathrm{K}$

$|I| < I_c$ → Constant phase difference $\varphi = \tilde{\varphi}_n = \arcsin\frac{I}{I_c} + 2\pi n$

$$\varphi = \tilde{\varphi}_n = \pi - \arcsin\left(\frac{I}{I_c}\right) + 2\pi n$$

→ Zero junction voltage → Zero-voltage state / ordinary (S) state

In practice → Junction + current source → Stability analysis

$E_{\mathrm{pot}} = E - F \cdot x$ → Potential energy of the system under action of external force

E → Intrinsic free energy of the junction

$F \leftrightarrow I$ → Generalized force

x → Generalized coordinate

$F \cdot \frac{\partial x}{\partial t} \leftrightarrow I \cdot V$ → Power flowing into subsystem

→ Tilted washboard potential

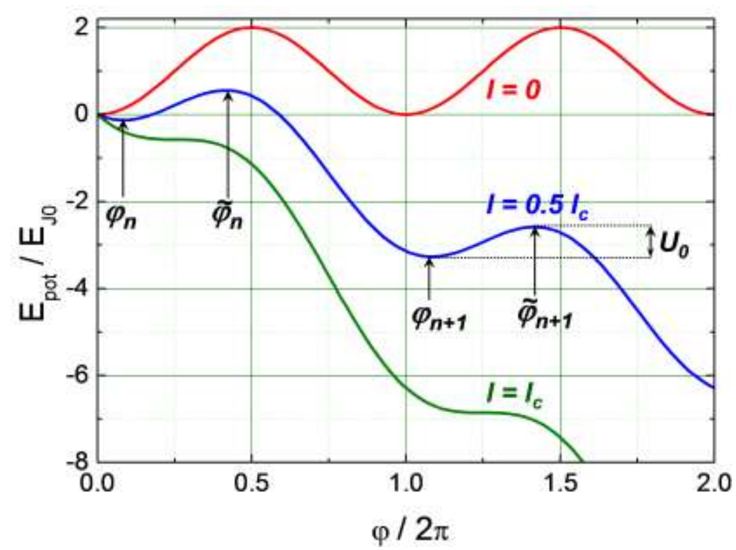

$$x \leftrightarrow \int V dt = \frac{\hbar}{2e}\varphi + c = \frac{\Phi_0}{2\pi}\varphi + c$$

→ Potential energy:

$$E_{\mathrm{pot}}(\varphi) = E_{\mathrm{J}} - I\left(\frac{\Phi_0}{2\pi}\varphi + c\right)$$

$$= E_{J0}\big(\underbrace{1 - \cos\varphi}_{\text{Junction (nonlinear)}} \underbrace{- \frac{I}{I_c}\varphi}_{\text{Source (linear)}}\big) + \tilde{c}$$

Stable minima φ_n

Unstable maxima $\tilde{\varphi}_n$

Equivalent states for different n

2.1.3 The superconducting state

Properties of the washboard potential

$$U_0 \equiv E_{\mathrm{pot}}(\varphi_{n+1}) - E_{\mathrm{pot}}(\widetilde{\varphi}_{n+1})$$
$$= 2E_{J0}\left[\sqrt{1-\left(\frac{I}{I_c}\right)^2} - \frac{I}{I_c}\arccos\left(\frac{I}{I_c}\right)\right]$$

$$k \equiv \frac{\partial^2 E_{\mathrm{pot}}}{\partial\varphi^2} = E_{J0}\sqrt{1-\left(\frac{I}{I_c}\right)^2}$$

$\rightarrow 0$ for $I \rightarrow I_c$

curvature at potential minimum

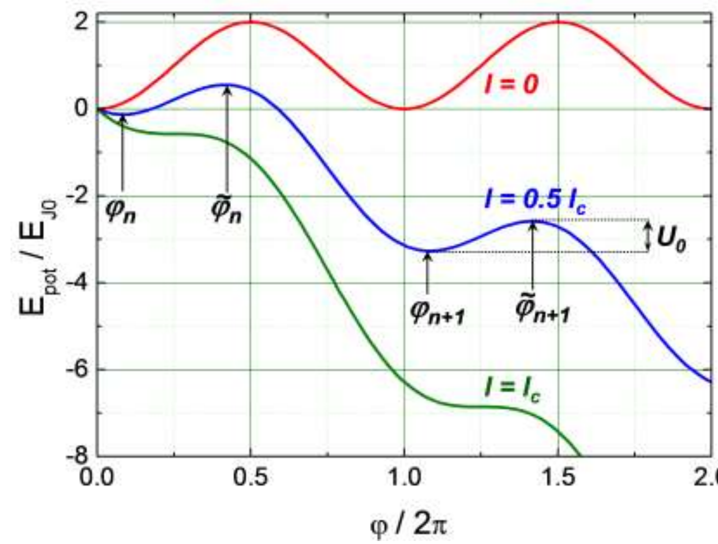

No minima for $I > I_c$

Close to I_c → $\alpha \equiv 1 - \frac{I}{I_c} \ll 1$ → Simplified approximations

$$\varphi_0 = \frac{\pi}{2} - \sqrt{2\alpha} \qquad \widetilde{\varphi}_0 = \frac{\pi}{2} + \sqrt{2\alpha} \qquad U_0 = \frac{2}{3}E_{J0}\,(2\alpha)^{2/3} \qquad k = E_{J0}\,(2\alpha)^{1/2}$$

Washboard potential extremely useful in describing junction dynamics for $I > I_c$

2.1.4 The Josephson inductance

Energy storage in JJ → Nonlinear reactance

$$\frac{dI_s}{dt} = I_c \cos\varphi \frac{d\varphi}{dt} \qquad \Rightarrow \frac{dI_s}{dt} = I_c \cos\varphi \frac{2\pi}{\Phi_0} V$$

$$I_s(t) = I_c \sin\varphi(t)$$

$$\frac{d\varphi}{dt} = \frac{2\pi}{\Phi_0} V$$

For small variations near $I_\mathrm{s} = I_\mathrm{c} \sin\varphi$ → JJ equivalent to inductance

$$\boxed{L_s = \frac{\Phi_0}{2\pi I_c \cos\varphi} = L_c \frac{1}{\cos\varphi}}$$

with $L_c = \frac{\hbar}{2eI_c}$ Josephson inductance

Properties of the Josephson inductance:

Negative for $\pi/2 + 2\pi n < \varphi < 3\pi/2 + 2\pi n$

($\mathrm{V} > 0$ → Oscillating Josephson current)

The pendulum analog

→ Plane mechanical pendulum in uniform gravitational field
→ Mass m, length ℓ, deflection angle θ
→ Torque D parallel to rotation axis
→ Restoring torque: $mg\ell\sin\theta$

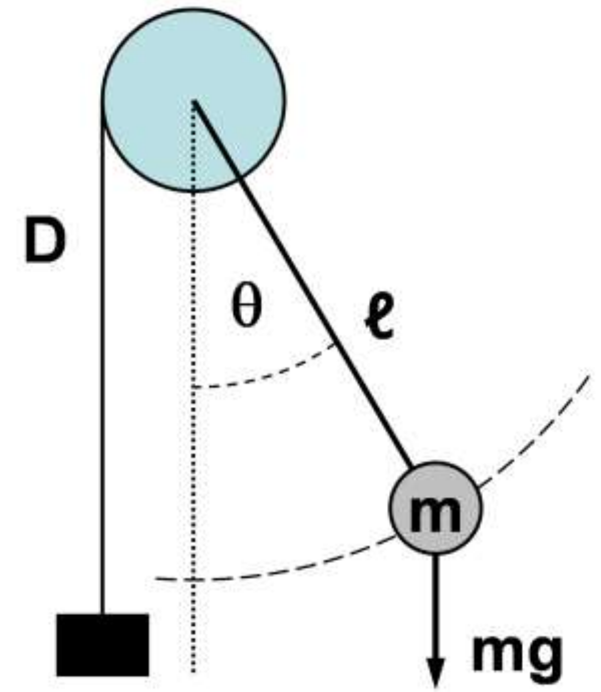

Equation of motion → $D = \Theta\ddot{\theta} + \Gamma\dot{\theta} + mg\ell\sin\theta$

$\Theta = m\ell^2$ Moment of inertia
Γ Damping constant

Analogies

$$I \leftrightarrow D$$
$$I_c \leftrightarrow mg\ell$$
$$\frac{\Phi_0}{2\pi R} \leftrightarrow \Gamma$$
$$\frac{C\Phi_0}{2\pi} \leftrightarrow \Theta$$
$$\varphi \leftrightarrow \theta$$

For $D = 0$ → Oscillations around equilibrium with

$$\omega = \sqrt{\frac{g}{\ell}} \leftrightarrow \text{Plasma frequency } \omega_p = \sqrt{\frac{2\pi I_c}{\Phi_0 C}}$$

Finite torque ($D > 0$) → Finite θ_0 → Finite, but constant φ_0 → Zero-voltage state

$$E_{\text{pot}}(\varphi) = E_{J0}\left[1 - \cos\varphi - \frac{I}{I_c}\varphi\right]$$

The washboard potential

Particle moving in tilted washboard potential $E_{\text{pot}}(\varphi) = E_{J0}\left(1 - \cos\varphi - \frac{I}{I_c}\varphi\right)$

→ Analogies

Coordinate x	$\leftrightarrow \varphi$	
Velocity v	$\leftrightarrow \frac{d\varphi}{dt} \propto V$	
Mass m	$\leftrightarrow$ Junction capacitance C	

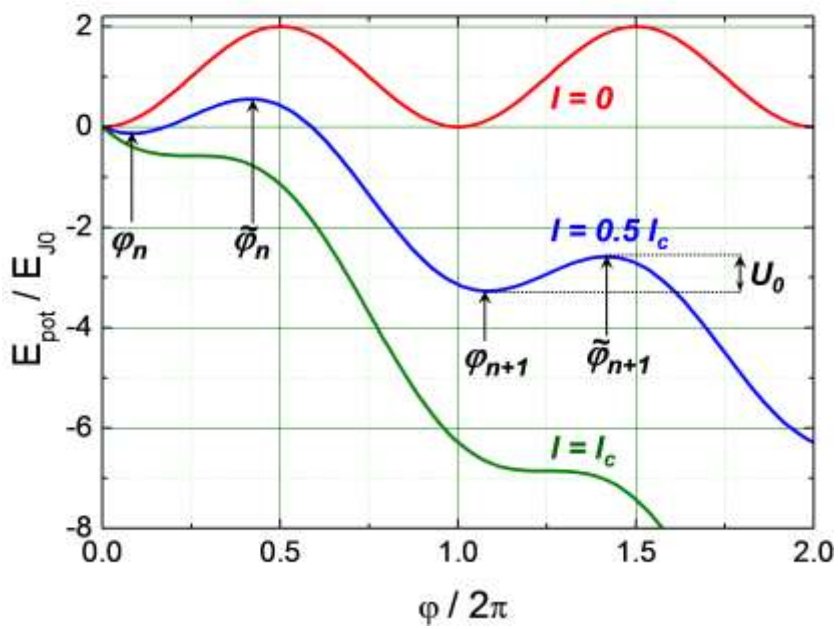

2.2 Short Josephson Junctions

So far: zero-dimensional JJ (lumped elements)

→ Homogeneous supercurrent density and phase difference

Now: extended junctions

→ Spatial variations $\boldsymbol{J}_{\mathbf{s}}(\boldsymbol{r})$ and $\varphi(\boldsymbol{r})$

→ Consider magnetic field generated by the Josephson current itself („self-field“)

Short Josephson junctions

→ Self-field small compared to external field

Long Josephson junctions

→ Self-field no longer negligible

Relevant length scale for transition from short to long Josephson junction:

Josephson penetration depth $\lambda_J = \sqrt{m_s/\mu_0 \underbrace{n_s}_{\text{density in weak coupling region}} q_s^2} \gg \lambda_L$

JJ at finite voltage → Temporal interference → Oscillation of Josephson current

JJ at finite phase gradient → Spatial interference → Magn. field dep. of Josephson current

External magnetic field
→ Spatial change of gauge invariant phase difference $\varphi(\boldsymbol{r})$
→ Spatial interference of macroscopic wave functions in JJ

Specific geometry

Insulating barrier thickness d

Junction area $A = L \times W$

Edge effects small: $W, L \gg d$

Electrode thickness $> \lambda_\mathrm{L}$

Ext. magnetic field $\boldsymbol{B}_\mathbf{e} = (0, B_y, 0)$

Magnetic thickness

$t_B = d + \lambda_{\mathrm{L},1} + \lambda_{\mathrm{L},2}$

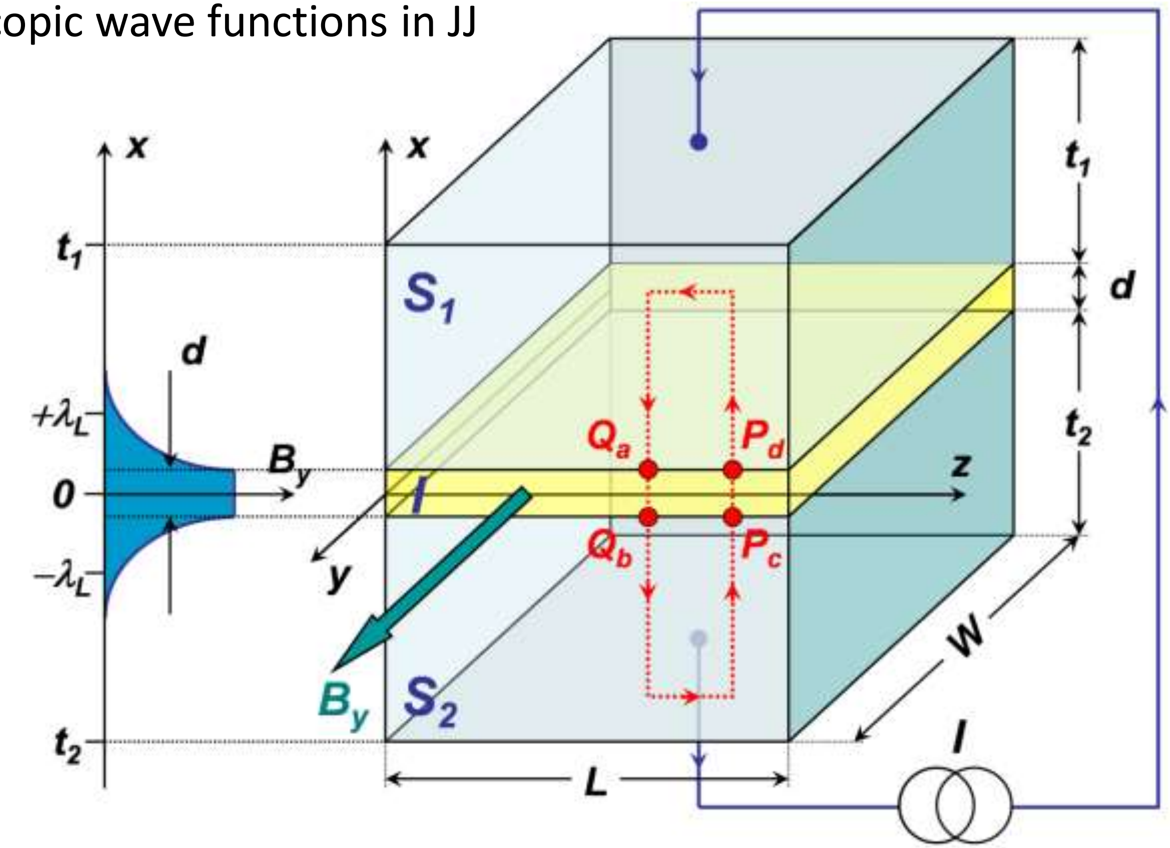

Effect of $\boldsymbol{B}_\mathbf{e}$ on $\boldsymbol{J}_\mathbf{s}$
→ Phase shift $\varphi(P) - \varphi(Q)$ between two points *P* and *Q* separated by *dz*
→ Line integral along red contour yields total phase change along closed contour

$$\oint_C \nabla\theta \cdot d\mathbf{l} = (\theta_{Q_b} - \theta_{Q_a}) + (\theta_{P_c} - \theta_{Q_b}) + (\theta_{P_d} - \theta_{P_c}) + (\theta_{Q_a} - \theta_{P_d}) = 0$$

1 2 3 4

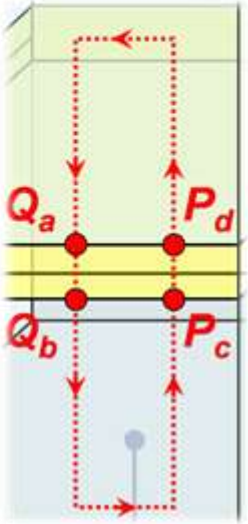

Gauge invariant phase gradient in the bulk superconductor:

$$\nabla\theta = \frac{2\pi}{\Phi_0}(\Lambda \mathbf{J}_s + \mathbf{A})$$

Gauge invariant phase difference across the barrier:

$$\varphi = \theta_2 - \theta_1 - \frac{2\pi}{\Phi_0}\int_1^2 \mathbf{A} \cdot d\mathbf{l}$$

1 & **3** are differences acrosss the junction:

$$\theta_{Q_b} - \theta_{Q_a} = +\varphi(Q) + \frac{2\pi}{\Phi_0}\int_{Q_a}^{Q_b} \mathbf{A} \cdot d\mathbf{l} \qquad \theta_{P_d} - \theta_{P_c} = -\varphi(P) + \frac{2\pi}{\Phi_0}\int_{P_c}^{P_d} \mathbf{A} \cdot d\mathbf{l}$$

2 & **4** differences in the bulk, supercurrent equation for $\nabla\theta$:

$$\theta_{P_c} - \theta_{Q_b} = \int_{Q_b}^{P_c} \nabla\theta \cdot d\mathbf{l} = \frac{2\pi}{\Phi_0}\int_{Q_b}^{P_c} \Lambda \mathbf{J}_s \cdot d\mathbf{l} + \frac{2\pi}{\Phi_0}\int_{Q_b}^{P_c} \mathbf{A} \cdot d\mathbf{l} \qquad \theta_{Q_a} - \theta_{P_d} = \int_{P_d}^{Q_a} \nabla\theta \cdot d\mathbf{l} = \frac{2\pi}{\Phi_0}\int_{P_d}^{Q_a} \Lambda \mathbf{J}_s \cdot d\mathbf{l} + \frac{2\pi}{\Phi_0}\int_{P_d}^{Q_a} \mathbf{A} \cdot d\mathbf{l}$$

Substitution →
$$\varphi(Q) - \varphi(P) = -\frac{2\pi}{\Phi_0}\oint_C \mathbf{A}\cdot d\mathbf{l} - \frac{2\pi}{\Phi_0}\int_{Q_b}^{P_c} \Lambda\mathbf{J}_s\cdot d\mathbf{l} - \frac{2\pi}{\Phi_0}\int_{P_d}^{Q_a} \Lambda\mathbf{J}_s\cdot d\mathbf{l}$$

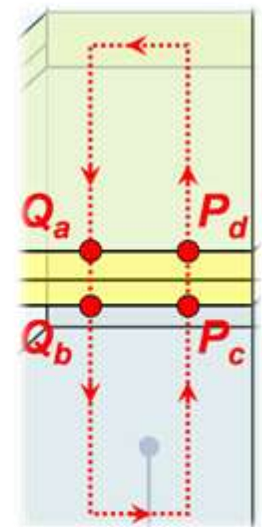

Integration of $\boldsymbol{A}$ around closed contour → Enclosed flux Φ

Integration of $\boldsymbol{J}_\mathbf{s}$ excludes insulating barrier → Incomplete contour C'

$$\oint_{C'} \Lambda\mathbf{J}_s\cdot d\mathbf{l} = \int_{Q_b}^{P_c} \Lambda\mathbf{J}_s\cdot d\mathbf{l} + \int_{P_d}^{Q_a} \Lambda\mathbf{J}_s\cdot d\mathbf{l}$$

Difference of gauge invariant phase differences $\varphi(Q) - \varphi(P)$

$$\varphi(Q) - \varphi(P) = -\frac{2\pi\Phi}{\Phi_0} - \frac{2\pi}{\Phi_0}\oint_{C'} \Lambda\mathbf{J}_s\cdot d\mathbf{l}$$

Line integral of supercurrent density $\boldsymbol{J}_\mathbf{s}$

→ Segments in *x*-direction cancel (separation: $dz \rightarrow 0$)

→ Segments in *z*-direction: deep inside SC ($> \lambda_\mathrm{L}$) → $\boldsymbol{J}_\mathbf{s}$ exponentially small

→ $$\varphi(P) - \varphi(Q) = \frac{2\pi\Phi}{\Phi_0} \qquad \frac{\varphi(P) - \varphi(Q)}{2\pi} = \frac{\Phi}{\Phi_0}$$

Total flux enclosed by the loop → $\Phi = B_y\underbrace{(d + \lambda_{L1} + \lambda_{L2})}_{\text{Magnetic thickness } t_B}dz = B_y t_B dz$

$$\varphi(P) - \varphi(Q) = \frac{2\pi\Phi}{\Phi_0}$$

$$\Phi = B_y(d + \lambda_{L1} + \lambda_{L2})dz = B_y t_B dz$$

$$\Rightarrow \varphi(P) - \varphi(Q) = \frac{2\pi}{\Phi_0} B_y t_B dz = \frac{\partial\varphi}{\partial z} dz$$

$$\Rightarrow \frac{\partial\varphi}{\partial z} = \frac{2\pi}{\Phi_0} B_y t_B$$

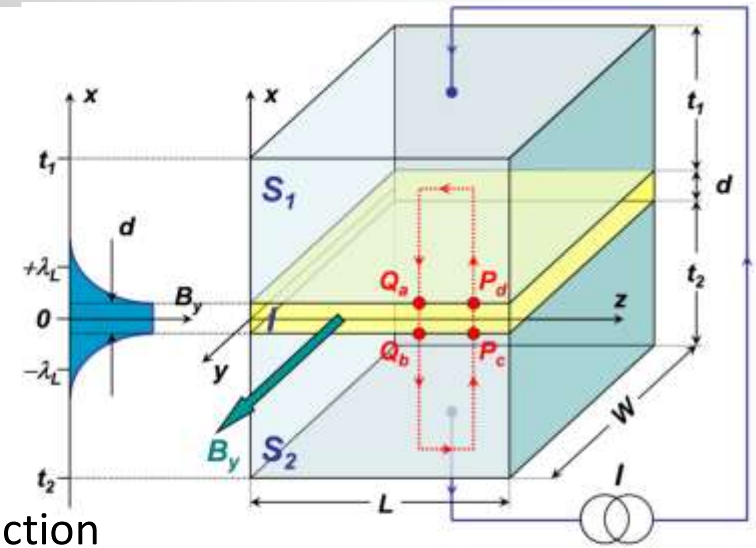

Similar argument for P and Q separated by dy in y-direction

$$\boxed{\nabla\varphi(\mathbf{r}, t) = \frac{2\pi}{\Phi_0} t_B \left[\mathbf{B}(\mathbf{r}, t) \times \hat{\mathbf{x}}\right]}$$

B-field component parallel to junction plane induces phase gradient

Integration gives: $$\varphi(z) = \frac{2\pi}{\Phi_0} B_y t_B z + \varphi_0$$

φ_0: phase difference at z = 0

Extended 1-st Josephson (current-phase) relation:

$$\boxed{J_s(y, z, t) = J_c(y, z) \sin\left(\frac{2\pi}{\Phi_0} t_B B_y z + \varphi_0\right) = J_c(y, z) \sin(kz + \varphi_0)}$$

with $$k = \frac{2\pi}{\Phi_0} t_B B_y$$

$\boldsymbol{J_s}$ varies periodically with period $\Delta z = \frac{2\pi}{k} = \frac{\Phi_0}{t_B B_y}$

Flux through the junction within one period: Φ_0

2.2.2 The Fraunhofer diffraction pattern

How does $I_s = \iint J_s(y,z)\,dy\,dz$ depend on the applied field $\boldsymbol{B}_{\mathbf{e}} = (0, B_y, 0)$?

Integration in *y*-direction: $i_c(z) = \int_{-W/2}^{W/2} J_c(y,z)\,dy$ $\qquad k = \frac{2\pi}{\Phi_0} t_B B_y$

$$\Rightarrow I_s(B_y) = \int_{-L/2}^{L/2} i_c(z) \sin(kz + \varphi_0)\, dz = \Im \left\{ e^{\imath\varphi_0} \int_{-\infty}^{\infty} i_c(z) e^{\imath kz} dz \right\}$$

Integral: complex, multiplication by $e^{\mathrm{i}\varphi_0}$ does not change magnitude

→ Magnitude yields maximum Josephson current

$$I_s^m(B_y) = \left| \int_{-\infty}^{\infty} i_c(z)\, e^{\imath kz} dz \right|$$

Magnetic field dependence of I_s^m

→ **Fourier transform** of $i_c(z)$

→ Analogy to optics

$J_c(y,z)$ homogeneous → $i_c(z)$ constant → Diffraction pattern of a slit → Fraunhofer pattern

$$I_s^m(\Phi) = I_c \left| \frac{\sin \frac{kL}{2}}{\frac{kL}{2}} \right| = I_c \left| \frac{\sin \frac{\pi\Phi}{\Phi_0}}{\frac{\pi\Phi}{\Phi_0}} \right|$$

$\Phi = B_y t_b L$ Flux though the junction

$I_c = i_c L$

Experimental observation of $I_s^m(\Phi)$ → Proof of Josephson tunneling of pairs

2.2.2 The Fraunhofer diffraction pattern

Spatially homogeneous maximum current density $J_c(y, z)$

→ Fraunhofer diffraction pattern

Maximum current density integrated along y-direction

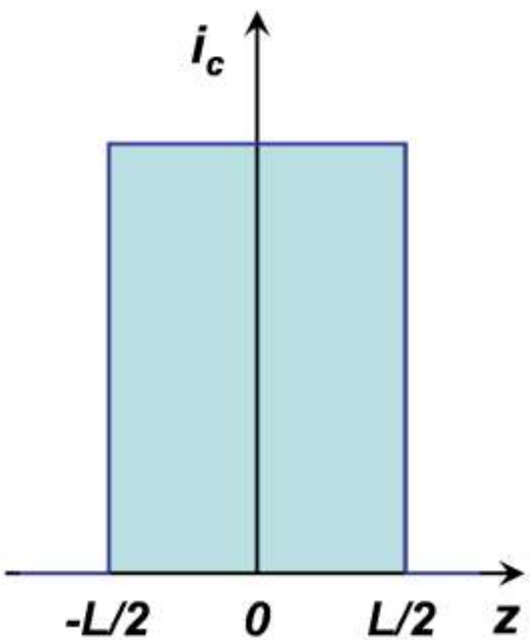

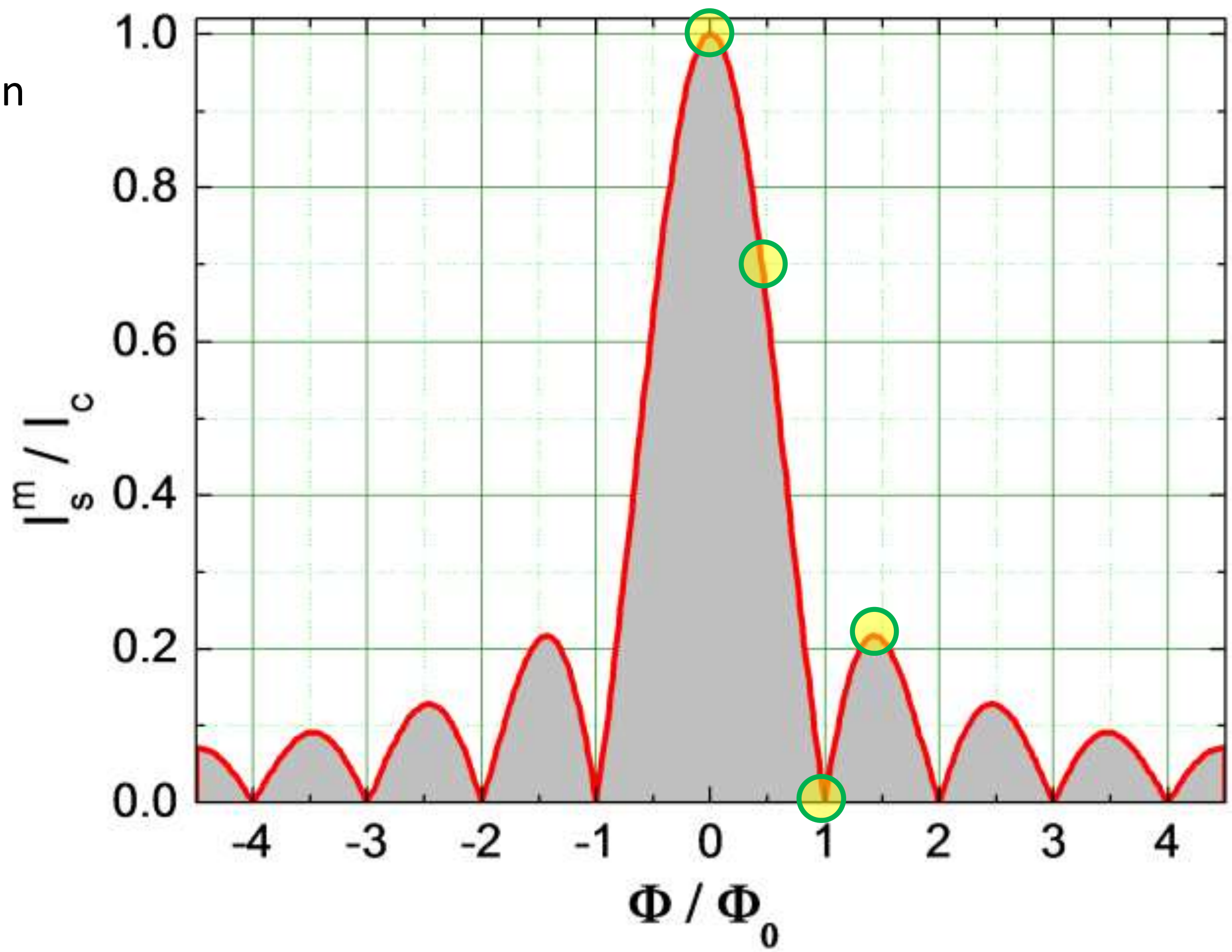

Experiment → Study the homogeneity of the supercurrent flow in JJ

2.2.2 The Fraunhofer diffraction pattern

Intepretation of the shape of $I_s^m(\Phi)$

→ **Spatial distribution** $i_s(z) = \int J_s(y,z)dy$
for different applied fields

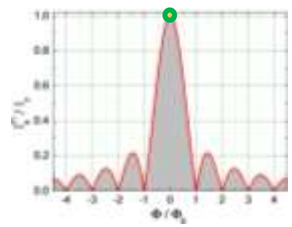

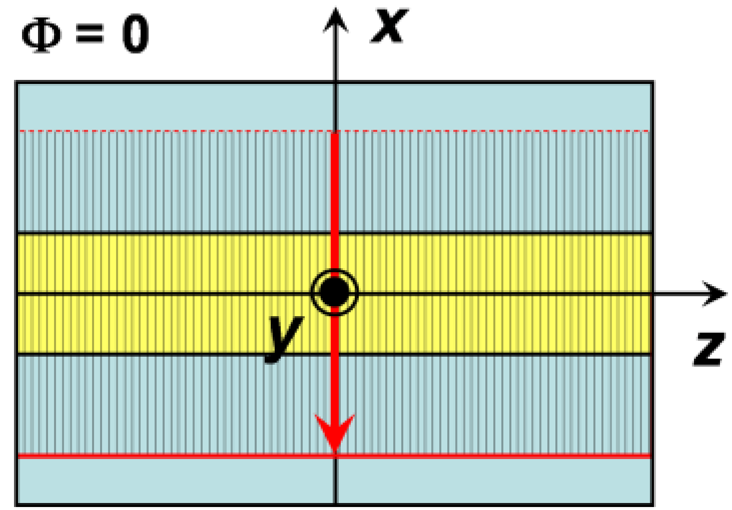

$\boldsymbol{\Phi = 0}$

→ $\varphi(z) = \varphi_0$

→ $i_s(z) = const.$

→ Josephson current maximum for $\varphi_0 = -\frac{\pi}{2}$

→ $J_s(y,z) = -J_c(y,z)$

$\boldsymbol{\Phi = \Phi_0/2}$

$$\varphi(z) = \frac{2\pi\Phi}{\Phi_0}\frac{z}{L} + \varphi_0 = \frac{\pi z}{L} + \varphi_0$$

→ Sinusoidal supercurrent variation with z
difference between edges:

$$\varphi(L/2) - \varphi(-L/2) = \pi$$

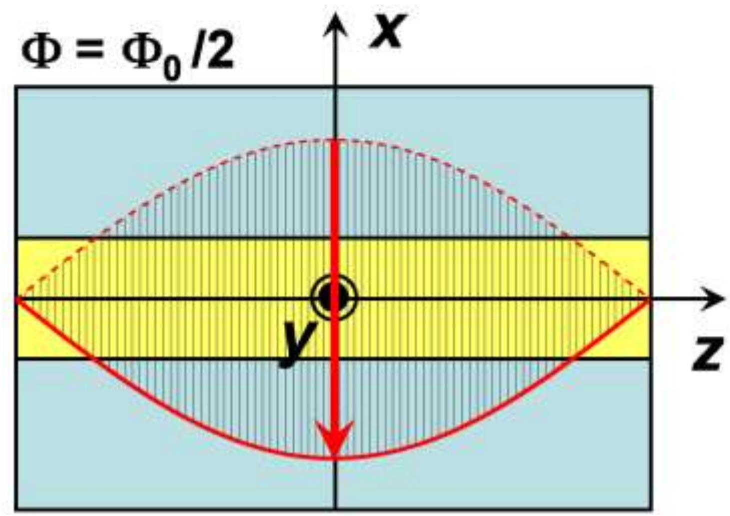

→ Half of an oscillation period

→ Josephson current maximum for $\varphi_0 = -\frac{\pi}{2}$

→ Linear increase of the phase from $-\pi$ at $z = -\frac{L}{2}$ to 0 at $z = +\frac{L}{2}$

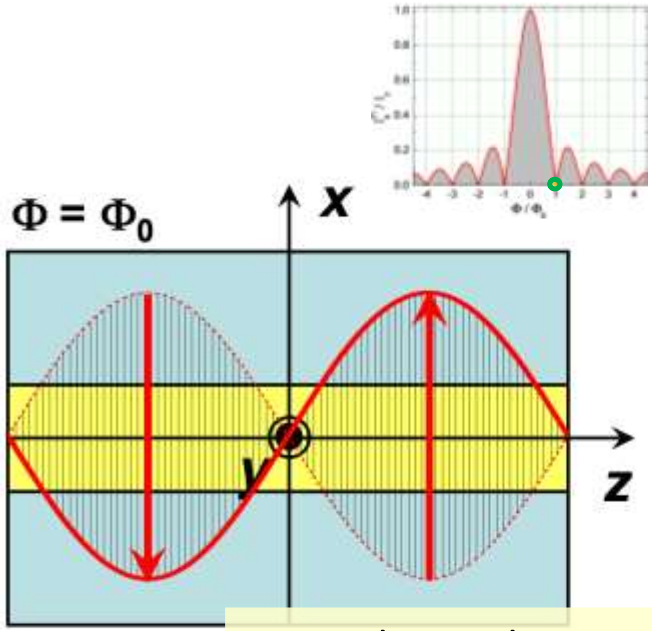

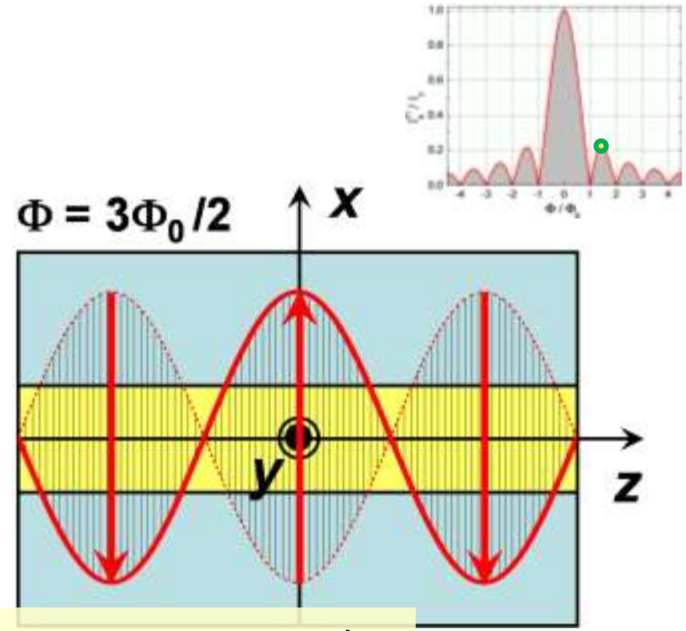

Local Josephson current density in negative and positive x-direction, but **no** net total current

→ Josephson current tends to decrease with increasing field

2.2.2 The Fraunhofer diffraction pattern

Spatial interference effect of macroscopic wave functions

→ Plane of constant phase in superconductor **2** is **tilted** by $\delta\varphi(z) = \frac{2\pi}{\Phi_0} B_y t_B z + \varphi_0$

here: destructive interference

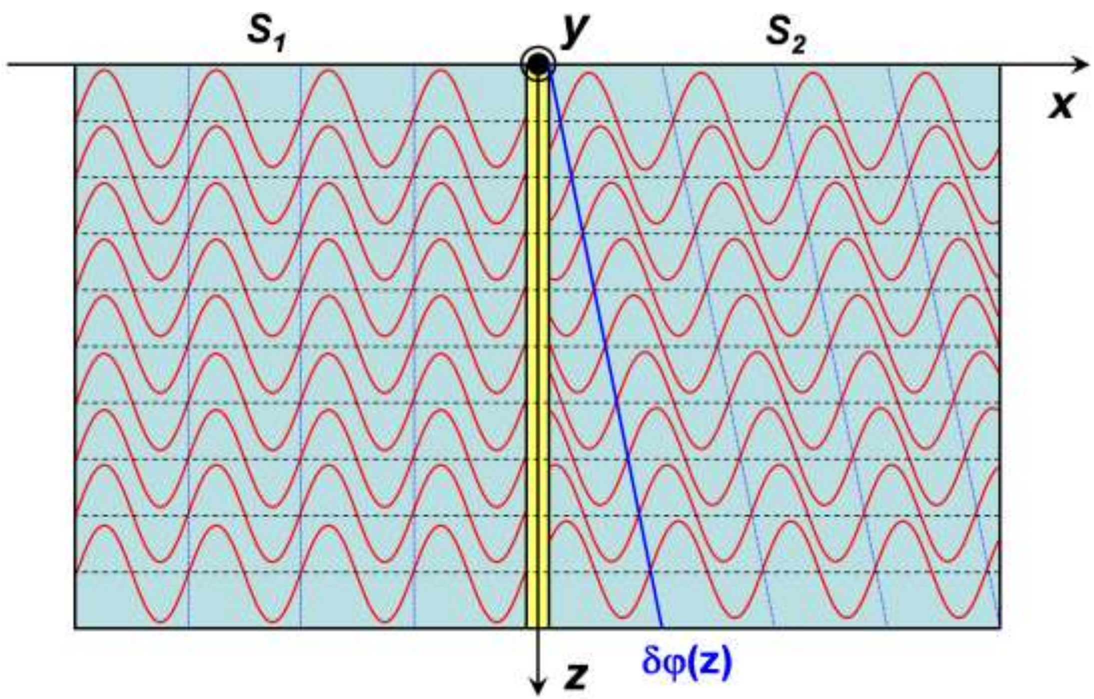

2.2.2 The Fraunhofer diffraction pattern

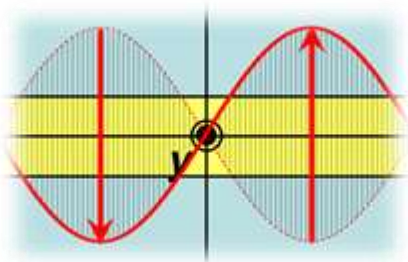

$\Phi = \Phi_0$

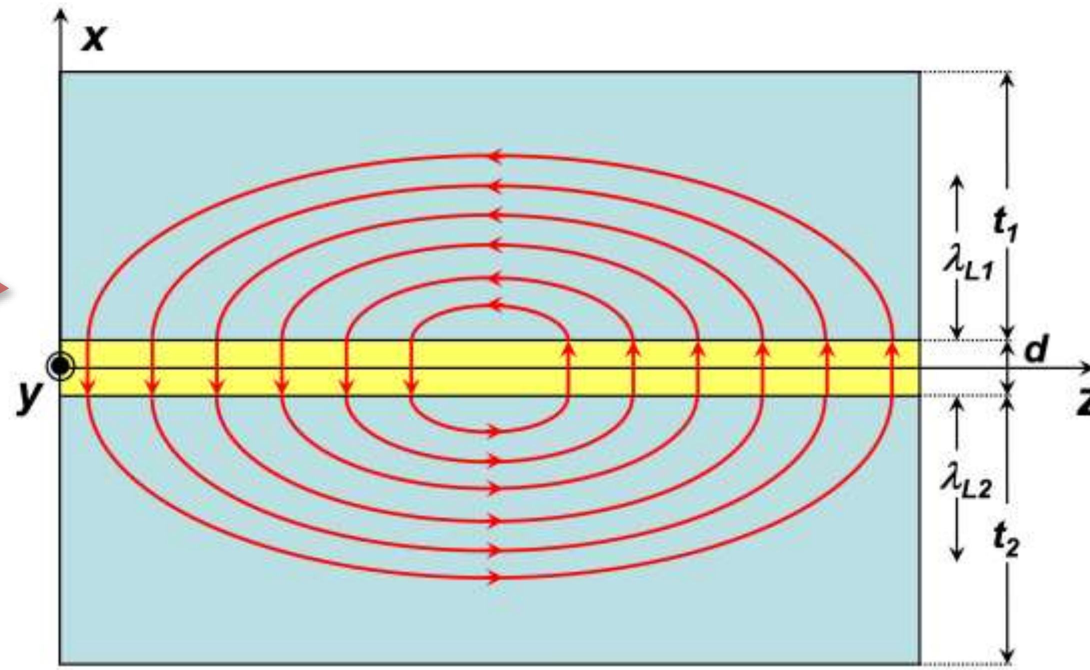

→ Closed current loop
→ No penetration of applied field into electrodes
→ **Josephson vortex**
→ No normal core because vortex core naturally in barrier region

2.2.2 The Fraunhofer diffraction pattern

Arbitrary direction of the applied field within barrier plane

$$\mathbf{B}_e = B_y\,\widehat{\mathbf{y}} + B_z\,\widehat{\mathbf{z}}$$

$$\Rightarrow I_s^m(\Phi) = I_c \left| \frac{\sin \frac{\pi\Phi_y}{\Phi_0}}{\frac{\pi\Phi_y}{\Phi_0}} \right| \left| \frac{\sin \frac{\pi\Phi_z}{\Phi_0}}{\frac{\pi\Phi_z}{\Phi_0}} \right|$$

$$\Phi_y = B_y t_b L \qquad \Phi_z = B_z t_b W$$

$$\Rightarrow I_s^m(\mathbf{B}_e) = \left| \int_S J_c(y,z) e^{\imath \mathbf{k}\cdot\mathbf{r}} dS \right|$$

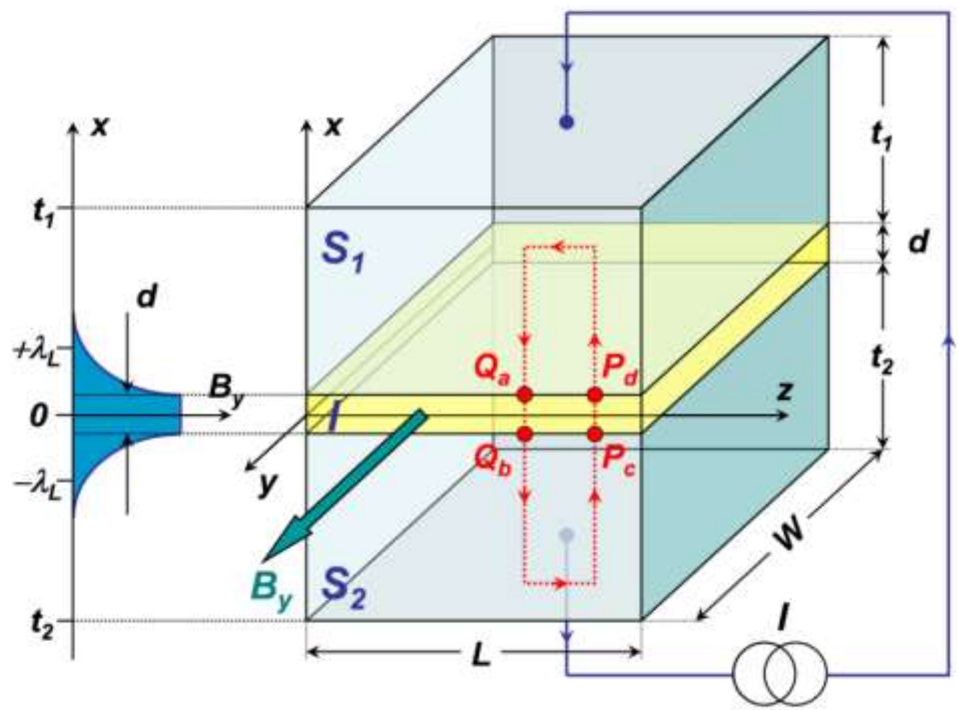

Inhomogeneous junctions

$$I_s^m(B_y) = \left| \int_{-\infty}^{\infty} i_c(z)\, e^{ikz}\, dz \right|$$

E.g., spatially varying barrier thickness

Experimental determination of $\boldsymbol{J}_{\mathbf{c}}(y,z)$ by measuring $I_s^{\mathrm{m}}(B)$?

→ No access via inverse Fourier transform
(Lack of phase information)

→ Approximate $I_c(z)$ under certain assumptions
Example → Symmetry to junction midpoint

$$i_c(z - L/2) = \frac{1}{\pi} \int_0^{\infty} |I_s^m(k)| \cos(kz)(-1)^{n(k)}\, dk \qquad k = \frac{2\pi}{\Phi_0} t_B B_y$$

$n \mathrel{\widehat{=}}$ number of zeros of $|I_s^{\mathrm{m}}(k)|$ between 0 and k

Spatial resolution

→ Information on $\boldsymbol{J}_{\mathbf{c}}(y,z)$ on small length scale?
→ Spatial resolution $\propto B_y^{-1}$

$$\frac{2\pi}{k} = \frac{\Phi_0}{t_B} \frac{1}{B_y} = L \frac{\Phi_0}{\Phi}$$

→ High B-fields required!
→ Spatial resolution for fields $\Phi \leq \Phi_0$ → Junction length L

Tailored junctions

Sometimes Frauenhofer sidelobes not desired (X-ray detectors)

→ Gaussian profile $i_c(z) = i_c(0)\ \exp\left(-\frac{z^2}{2\sigma^2}\right)$

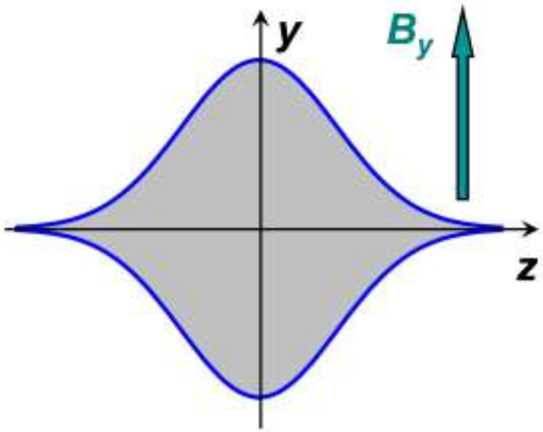

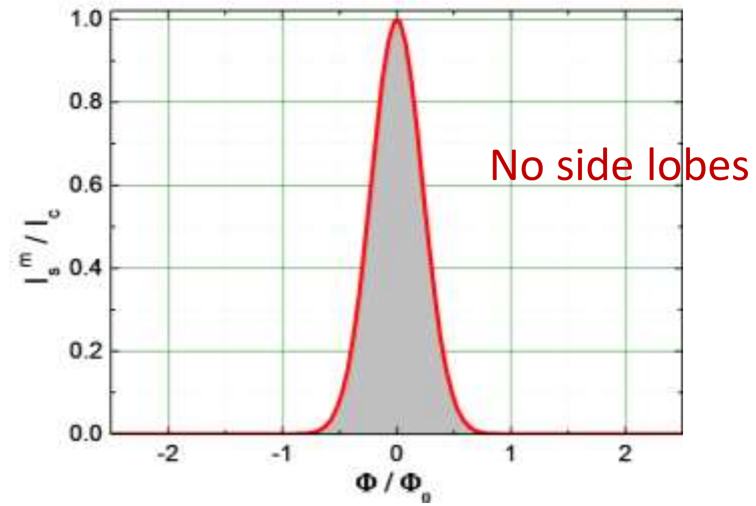

→ Junction shape should approach Gauss curve for homogeneous $\boldsymbol{J_c}(y, z)$

→ Integrated current density in y-direction $i_c(z) = \int J_c(y, z) dy$ → Gaussian profile

$$I_s^m(\Phi) = \sqrt{\frac{1}{2\pi}} i_c(0) L \exp\left(-\sigma k^2\right) = \sqrt{\frac{1}{2\pi}}\ i_c(0) L \exp\left(-\sigma \frac{4\pi^2}{L^2} \frac{\Phi^2}{\Phi_0^2}\right)$$

2.2.3 Additional topic:
Determination of the maximum Josephson current density

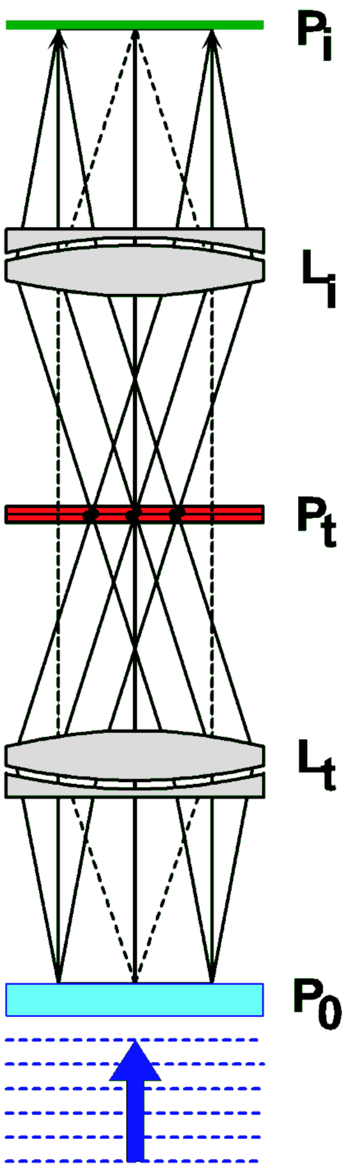

Additional topic: Supercurrent auto-correlation function

Comparison

Optical diffraction experiment	Field dependence of max. Josephson current
Transmission function $P_0(z)$	$i_c(z)$
Square root of light intensity P_t in focal plane	$I_s^{\mathrm{m}}(B_y)$
BackTransform → P_i (spatial resolution given by number of diffraction orders)	Phase is lost → BackTransform of intensity $(I_c^{\mathrm{m}})^2(B_y)$ → Autocorrelation function of the supercurrent distribution

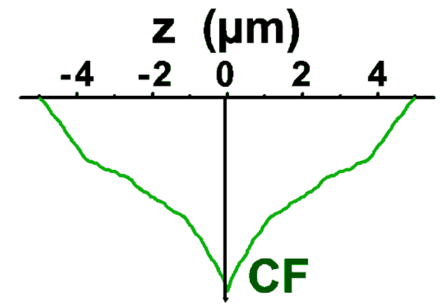

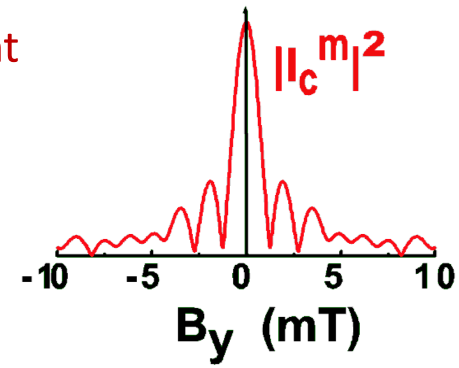

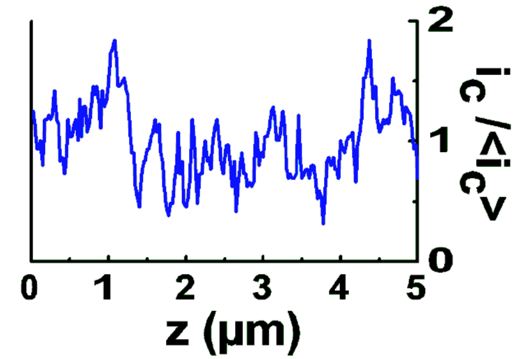

2.2.3 Additional topic: Determination of the maximum Josephson current density

Definition of auto-correlation function

$$\mathrm{AC}(\delta) = \int_{-\infty}^{\infty} i_c(z) i_c(z+\delta) dz$$

→ Overlap of $i_c(z)$ with itself, but shifted by δ

Wiener-Khinchine theorem

→ Autocorrelation function of $i_c(z)$:

$$\mathrm{AC}(\delta) = \int_{-\infty}^{\infty} |I_s^m(k)|^2 \, e^{ik\delta} dk$$

$$k = \frac{2\pi}{\Phi_0} t_B B_y = \frac{1}{L} 2\pi \frac{\Phi}{\Phi_0}$$

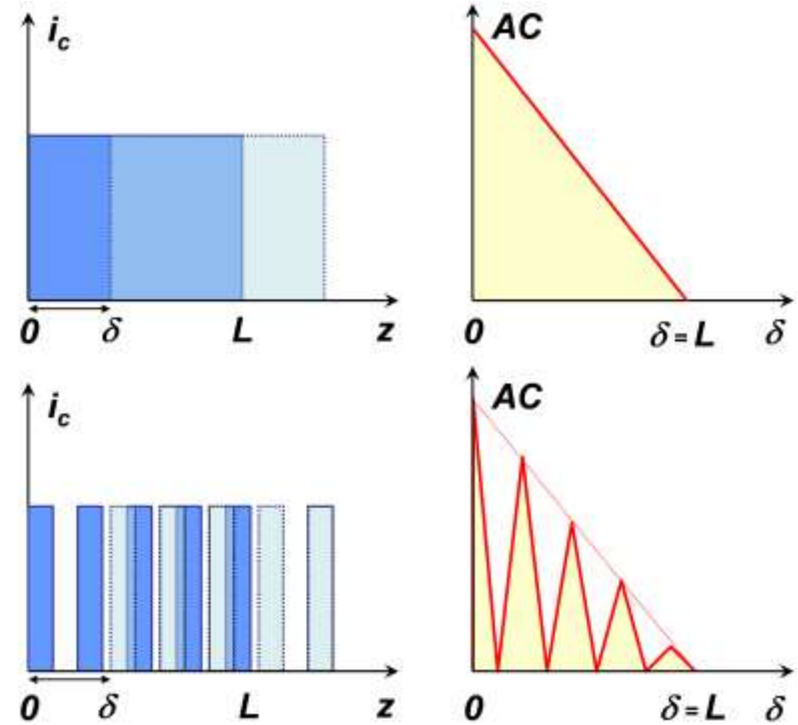

Spatial information contained in AC-function depends on magnetic field interval

spatial resolution $\quad 2\pi/k = L\dfrac{\Phi_0}{\Phi}$

Record 100 lobes in $I_s^{\mathrm{m}}(B_y)$ → Spatial resolution $0.01 \times$ junction width

→ Statistical information in envelope of $\left|I_s^{\mathrm{m}}(B_y)\right|^2$

2.2.3 Additional topic:
Determination of the maximum Josephson current density

Prototypical examples:

→ Inhomogeneities with probability $p(a) \propto 1/a \leftrightarrow p \times a = const.$)

→ $\left|I_s^m(B_y)\right|^2 \propto B_y^{-1}$

→ „Spatial 1/f noise“

→ Random distribution of filaments with width a:

→ Envelope constant up to $k = \frac{2\pi}{a}$

→ $\left|I_s^m(B_y)\right|^2 \propto B_y^{-2}$

→ „Spatial shot noise“

Analysis of autocorrelation function gives statistical information on current density inhomogeneities

$YBa_2Cu_3O_{7-\pm}$ grain boundary JJ

Slope of envelop is -0.65

→ $\left|I_s^m(B_y)\right|^2 \propto B_y^{-1.3}$

→ $p(a) \propto \frac{1}{a^{1.5}}$

→ Small scale inhomogeneities are more probable

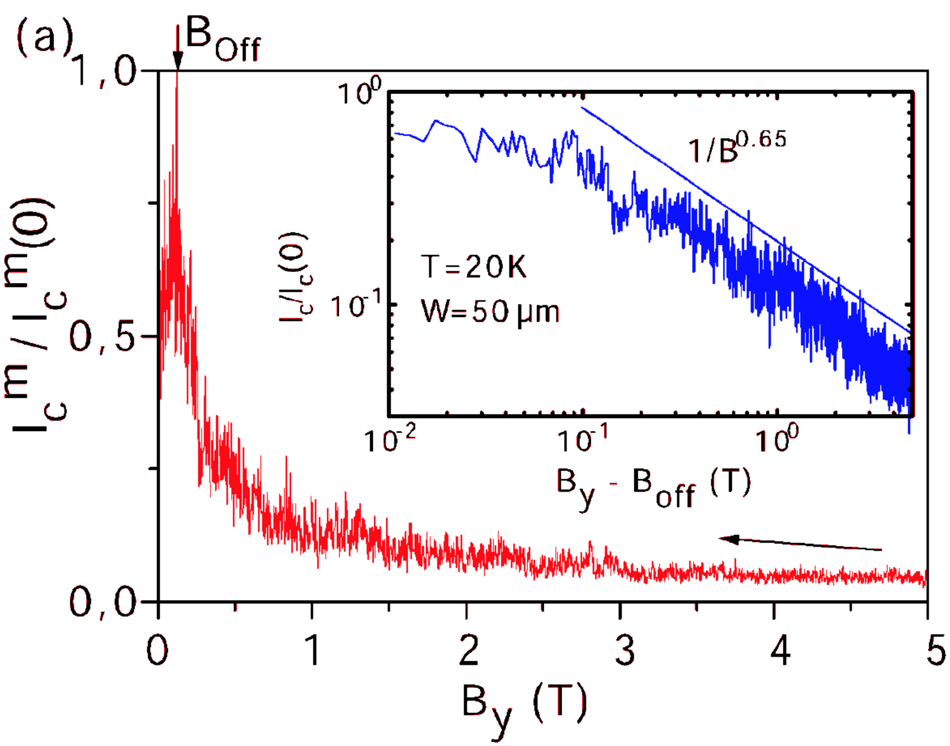

Scanning of JJ by focused electron / laser beam

→ Measure change $\delta I_{\mathrm{s}}^{\mathrm{m}}(y,z)$ as function of beam position (y,z)

→ $\delta I_{\mathrm{s}}^{\mathrm{m}}(y,z) \propto J_{\mathrm{c}}(y,z)$ → 2D image of $J_{\mathrm{c}}(y,z)$

→ Spatial resolution ≈ thermal healing length (≈ $1\ \mu\mathrm{m}$)

2.2.6 The motion of Josephson vortices

Josephson vortices

→ Visualize Josephson current density

→ Vortices **moving** in z-direction at constant speed v_z

→ Short junction

→ Self-field negligible

→ Flux density in junction given by $\boldsymbol{B}_{\mathbf{e}} = (0, B_y, 0)$

→ Gauge invariant phase difference

$$\frac{\partial \varphi}{\partial z} = \frac{2\pi}{\Phi_0} B_y t_B$$

$$\Phi = B_y t_B z$$

→ Passage of 1 vortex changes phase by 2π

$$\frac{\partial \varphi}{\partial t} = \frac{2\pi}{\Phi_0}\frac{\partial \Phi}{\partial t} = \frac{2\pi}{\Phi_0} B_y t_B \frac{\partial z}{\partial t} = \frac{2\pi}{\Phi_0} B_y t_B v_z$$

$$\Rightarrow \varphi(z,t) = \frac{2\pi}{\Phi_0} B_y t_B (z - v_z t) + \varphi(0)$$

$$= k(z - v_z t) + \varphi(0)$$

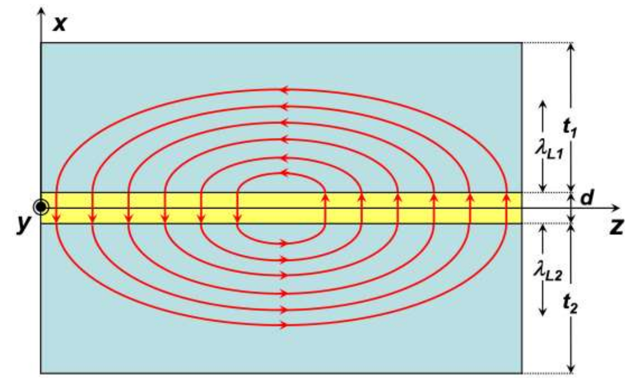

$\Phi = \Phi_0$

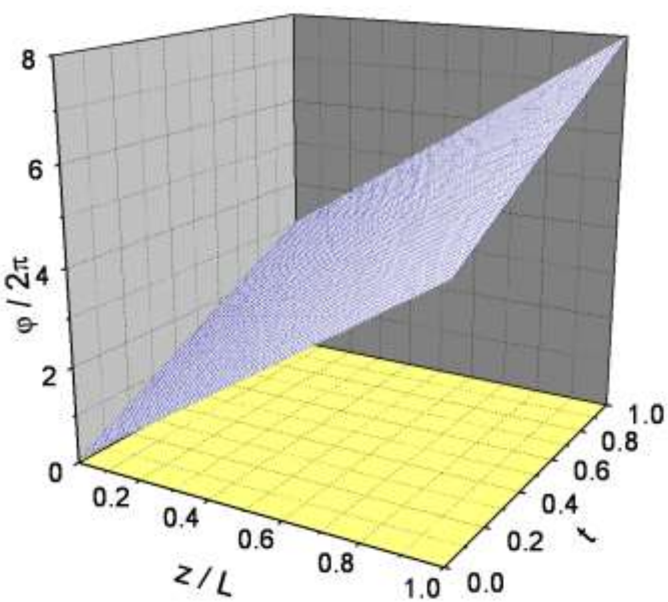

2.2.6 The motion of Josephson vortices

$J_s(y,z,t) = J_c(y,z)\sin(kz+\varphi_0)$

$$\Rightarrow J_s(y,z,t) = J_c(y,z)\sin[k(z - v_z t)]$$

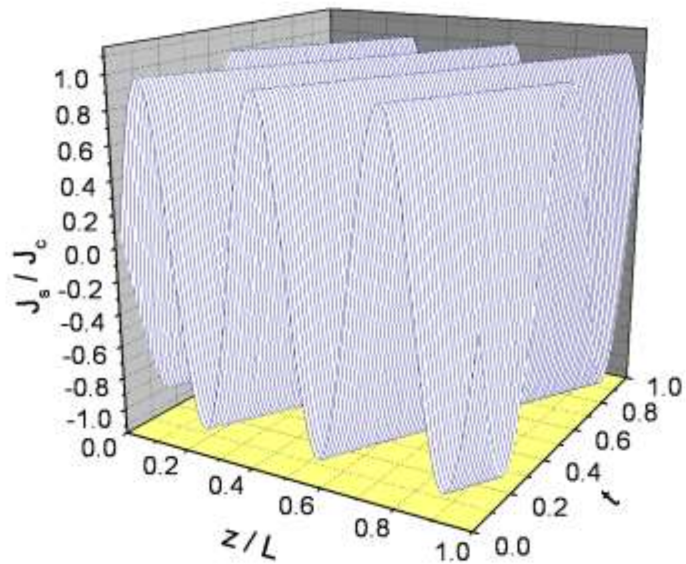

→ Current density pattern: moves at v_z

→ Vortex with period $p = L\frac{\Phi_0}{\Phi}$

→ Number of vortices in junction

$$N_V = \frac{L}{p} = \frac{\Phi}{\Phi_0}$$

→ Change of gauge-invariant phase difference

$$\Delta\varphi = 2\pi\frac{\Phi}{\Phi_0} = 2\pi N_V$$

$2\pi \times$ # of vortices

2.2.6 The motion of Josephson vortices

→ Rate of vortex passage

$$\frac{dN_V}{dt} = \frac{1}{2\pi}\frac{d\Delta\varphi}{dt}$$

with the voltage-phase relation

$$\frac{d\varphi}{dt} = \frac{2\pi}{\Phi_0} V$$

$$\frac{dN_V}{dt} = \frac{V}{\Phi_0}$$

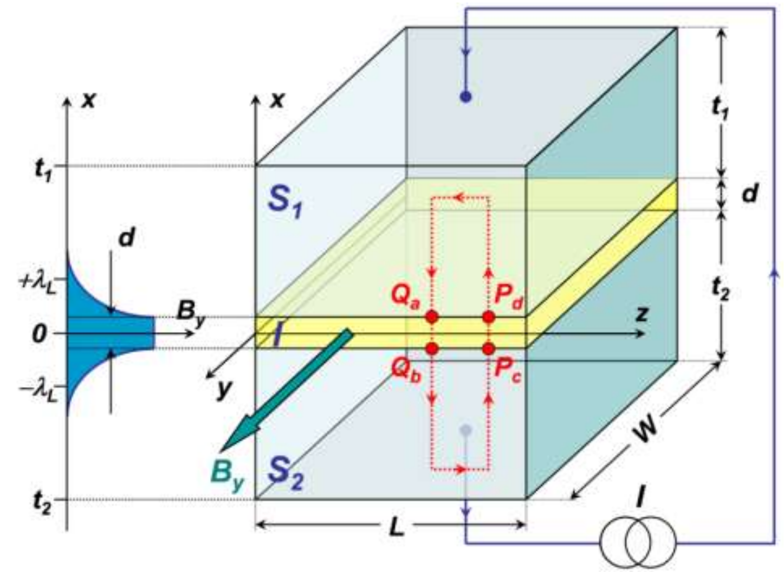

Constant velocity of vortices → Constant junction voltage / vortex rate

→ Application

→ Single flux quantum pump

→ Pump frequency $f = \frac{dN_v}{dt}$ → $V = f \cdot \Phi_0$

2.2 Summary – Short Josephson Junctions

→ Short JJ = lateral junction dimensions small compared to Josephson penetration depth

→ Effect of magnetic field parallel to junction electrodes

phase gradient $$\nabla\varphi(\mathbf{r},t) = \frac{2\pi}{\Phi_0} t_B \left[\mathbf{B}(\mathbf{r},t) \times \hat{\mathbf{x}}\right]$$

Josephson current density $$J_s(y,z,t) = J_c(y,z)\sin\left(\frac{2\pi}{\Phi_0} t_B B_y z + \varphi_0\right)$$

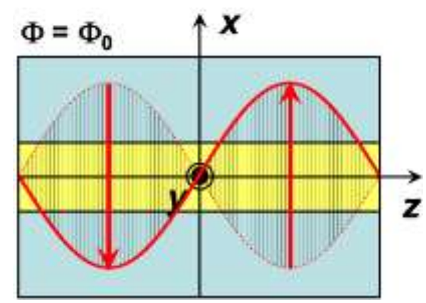

→ Spatial distribution of $i_s(z) = \int J_s(y,z)dy$

→ Josephson vortex

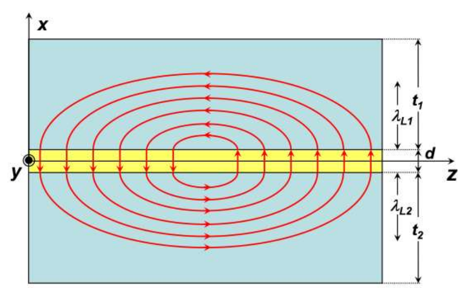

2.2 Summary – Short Josephson Junctions

→ Magnetic field dependence of maximum Josephson current $I_s^m(B_y) = \left| \int_{-\infty}^{\infty} i_c(z) e^{ikz} dz \right|$

$$I_s^m(\Phi) = I_c \left| \frac{\sin \frac{kL}{2}}{\frac{kL}{2}} \right| = I_c \left| \frac{\sin \frac{\pi\Phi}{\Phi_0}}{\frac{\pi\Phi}{\Phi_0}} \right|$$

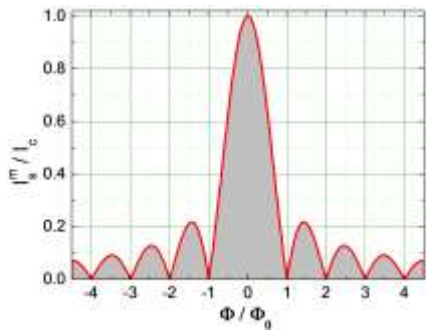

$$k = \frac{2\pi}{\Phi_0} t_B B_y$$

$$I_c = i_c L$$

Fraunhofer diffraction pattern

→ Analogy to single slit diffraction in optics, but no inverse Fourier transform (missing phase)

Autocorrelation function

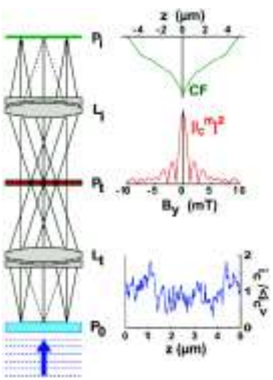

→ Motion of Josephson vortices
Motion of single vortex across junction results in phase change of 2π

$$V \propto \frac{\partial\varphi}{\partial t} = \frac{2\pi}{\Phi_0}\frac{\partial\Phi}{\partial t} = \frac{2\pi}{\Phi_0} B_y t_B \frac{\partial z}{\partial t} = 2\pi \frac{\Phi}{\Phi_0}\frac{v_z}{L}$$

Constant motion of vortices → Constant junction voltage / vortex rate

2.3.1 The stationary Sine-Gordon equation

$$\frac{\partial \varphi}{\partial z} = \frac{2\pi}{\Phi_0} B_y t_B \,, \quad \nabla\varphi(\mathbf{r},t) = \frac{2\pi}{\Phi_0} t_B \left[\mathbf{B}(\mathbf{r},t) \times \hat{\mathbf{x}}\right]$$

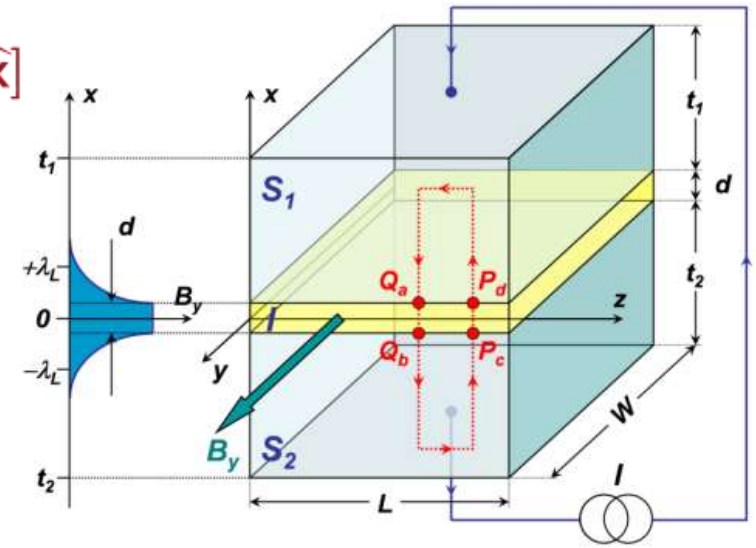

Now → Magnetic flux density given by
external **and** self-generated field

Ampere's law → $\nabla \times \mathbf{B} = \mu_0 \mathbf{J} + \epsilon\epsilon_0\mu_0 \frac{\partial \mathbf{E}}{\partial t}$

Zero-voltage state: $$\frac{\partial B_y(z)}{\partial z} = -\mu_0 J_x(z)$$

Spatial derivative: $$\frac{\partial^2 \varphi(z)}{\partial z^2} = \frac{2\pi t_B}{\Phi_0}\frac{\partial B_y(z)}{\partial z} = -\frac{2\pi\mu_0 t_B}{\Phi_0} J_x(z)$$

Assume $J_c(y,z) = const.$ and use $J_x(y,z) = -J_s(y,z)$ → $J_x(z) = -J_c \sin\varphi(z)$

$$\boxed{\frac{\partial^2 \varphi(z)}{\partial z^2} = \frac{2\pi\mu_0 t_B J_c}{\Phi_0} \sin\varphi(z) = \frac{1}{\lambda_J^2} \sin\varphi(z)}$$

Stationary Sine-Gordon equation (SSGE)
(nonlinear differential equation)

Josephson penetration depth $\lambda_J \equiv \sqrt{\frac{\Phi_0}{2\pi\mu_0 t_B J_c}}$

Two-dimensional stationary Sine-Gordon equation

$$\boxed{\frac{\partial^2\varphi(y,z)}{\partial y^2}+\frac{\partial^2\varphi(y,z)}{\partial z^2}=\frac{1}{\lambda_J^2}\sin\varphi(y,z)}$$

Relation between London and Josephson penetration depth

$$\lambda_L \equiv \sqrt{\frac{m_s}{\mu_0 n_s q_s^2}} \Longleftrightarrow \lambda_J \equiv \sqrt{\frac{\Phi_0}{2\pi\mu_0 t_B J_c}}$$

with $\mathbf{J}_s = q_s n_s \left\{\frac{\hbar}{m_s}\nabla\theta(\mathbf{r},t) - \frac{q_s}{m_s}\mathbf{A}(\mathbf{r},t)\right\} \Rightarrow \mathbf{J}_c \simeq q_s n_s^\star \frac{\hbar}{m_s}\frac{2\pi}{t_B}$

insert into expression for Josephson penetration depth

$$\lambda_J = \sqrt{\frac{\Phi_0}{2\pi\mu_0 t_B J_c}} \approx \sqrt{\frac{\hbar}{q_s\mu_0 t_B}\frac{m_s t_B}{2\pi\hbar q_s n_s^\star}} = \sqrt{\frac{m_s}{2\pi\mu_0 n_s^\star q_s^2}} \approx \lambda_L(n_s^\star)$$

→ λ_J corresponds to the London penetration depth of the weak coupling region with reduced superelectron density $n_s^\star$

2.3.1 The stationary Sine-Gordon equation

Small φ → Linearization: $\sin\varphi \approx \varphi$ → $$\frac{\partial^2\varphi(z)}{\partial z^2} = \frac{1}{\lambda_J^2}\varphi(z) \quad \Rightarrow \varphi(z) = \varphi(0)e^{-z/\lambda_J}$$

Magnetic field along the junction $$\Rightarrow B_y(z) = -\frac{\varphi(0)}{2\pi}\frac{\Phi_0}{\lambda_J t_B}e^{-z/\lambda_J}$$

$$\frac{\partial\varphi}{\partial z} = \frac{2\pi}{\Phi_0}B_y t_B$$

→ λ_J is a decay length

with $$\frac{\partial B_y(z)}{\partial z} = -\mu_0 J_x(z) \quad \Rightarrow J_x(z=0) = \frac{1}{\lambda_J}\frac{B_y(z=0)}{\mu_0}$$

→ Current flows at the edges of the junction

→ Meißner solution, possible for $J_x < J_c$ or $B_y(z=0) \leq \mu_0 J_c \lambda_J$

Small junction $L \ll \lambda_J$ → $$\frac{\partial^2\varphi(z)}{\partial z^2} \simeq 0 \Rightarrow \frac{\partial\varphi(z)}{\partial z} \simeq \text{const}$$ → **Short junction result**

2.3.2 The Josephson vortex

Particular solution of the SSGE:

$$\varphi(z) = \pm 4 \arctan\left\{\exp\left(\frac{z - z_0}{\lambda_J}\right)\right\} + 2\pi n$$

$$\frac{\partial \varphi}{\partial z} = \frac{2\pi}{\Phi_0} B_y t_B$$

$$B_y(z) = \pm \frac{\Phi_0}{\pi \lambda_L t_B} \frac{1}{\cosh\left(\frac{z-z_0}{\lambda_J}\right)}$$

$$\frac{\partial^2 \varphi(z)}{\partial z^2} = -\frac{2\pi \mu_0 t_B}{\Phi_0} J_x(z)$$

$$J_x(z) = -J_s(z) = \pm \frac{\Phi_0}{\pi \mu_0 \lambda_L^2 t_B} \frac{\sinh\left(\frac{z-z_0}{\lambda_J}\right)}{\cosh\left(\frac{z-z_0}{\lambda_J}\right)} = \pm 2 J_c \frac{\sinh\left(\frac{z-z_0}{\lambda_J}\right)}{\cosh\left(\frac{z-z_0}{\lambda_J}\right)}$$

General solution: particular + homogeneous solution

→ Important case: junction of infinite length, $\frac{d\varphi}{dz}$ vanishes for $z \to \pm\infty$

→ Particular solution = Complete solution

2.3.2 The Josephson Vortex

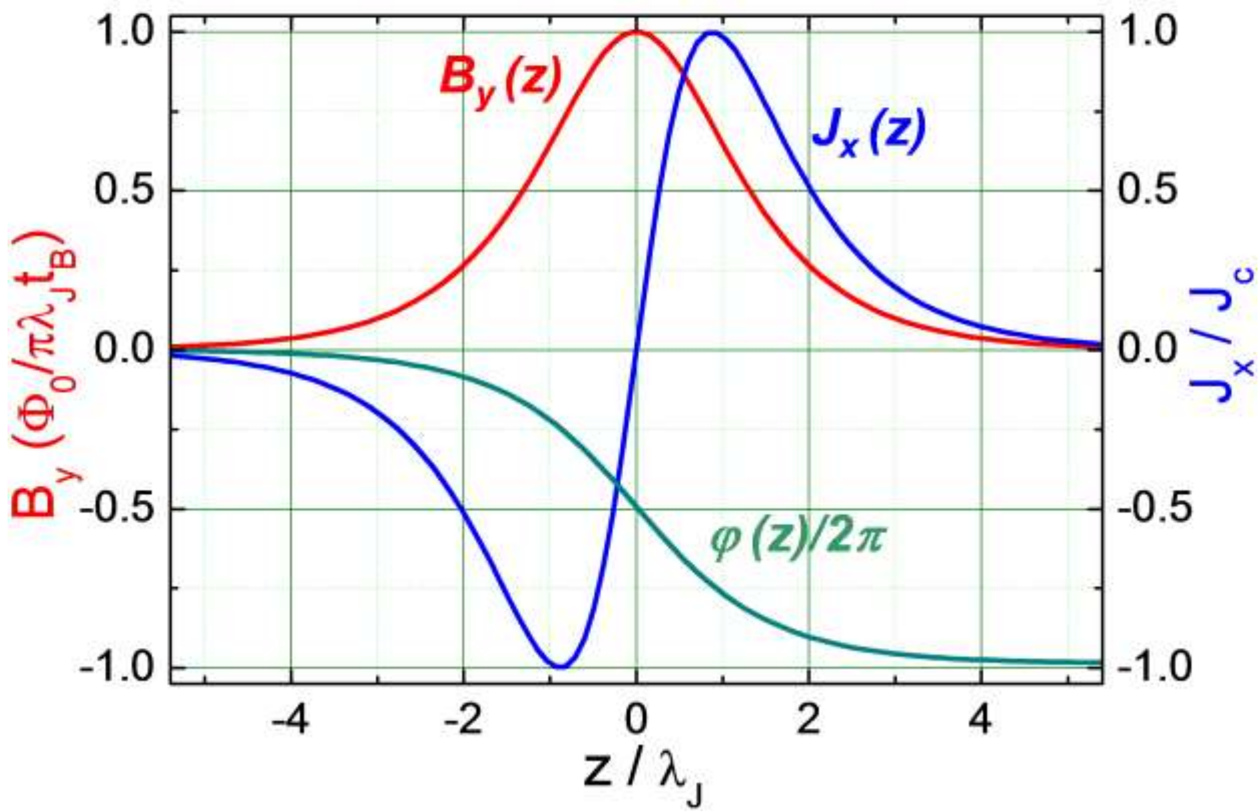

Decay length for $J_s$and B_y → λ_J

Maximum of J_s does not coincide with maximum of B_y

Integration

→ Total current $= 0$

→ Total flux $= \Phi_0$

→ Josephson vortex in an infinitely long junction

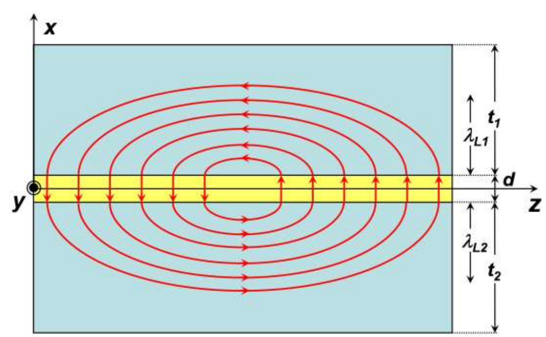

2.3.2 The Josephson vortex

Energy per unit length of vortex:

$$E = \frac{1}{2\mu_0}\int_{V_s+V_i} \mathbf{B}^2 dV + \int_{A_i} \frac{\Phi_0 J_c(y,z)}{2\pi}[1-\cos\varphi(z)]dydz$$

$$E_{\text{Vortex}} = \frac{E_l}{W} = \frac{4\Phi_0 J_c \lambda_J}{\pi}$$

→ $E_{\text{Vortex}} > 0$ → We need external field and/or current to supply energy

Magnetic flux density B_{c1} for first vortex entrance:

$$B_{c1} = \frac{\mu_0}{\Phi_0} E_{\text{Vortex}}$$

$$B_{c1} = \frac{\mu_0}{\Phi_0} E_{\text{Vortex}} = \frac{4\mu_0 J_c \lambda_J}{\pi} = \frac{2\Phi_0}{\pi^2 \lambda_J t_B}$$

$B_{c1} \approx$ Magnetic flux density of a single flux quantum distributed over an area $t_B \times \lambda_J$

Here: Infinitely long junction

→ Simple & Prototypical case (boundary conditions not relevant)

→ Reveals relevant physical principles

→ Real junctions → Boundary conditions → Complex vortex dynamics!

2.3.3 Junction types and boundary conditions

Junction geometry determines current flow → Boundary conditions of SSGE

→ Magnetic flux density at junction edges:

$$\frac{\partial^2\varphi(y,z)}{\partial y^2} + \frac{\partial^2\varphi(y,z)}{\partial z^2} = \frac{1}{\lambda_J^2}\sin\varphi(y,z)$$

$$\left.\frac{\partial\varphi}{\partial z}\right|_{z=0} = \left.\frac{2\pi t_B}{\Phi_0}B_y\right|_{z=0} \qquad \left.\frac{\partial\varphi}{\partial z}\right|_{z=L} = \left.\frac{2\pi t_B}{\Phi_0}B_y\right|_{z=L}$$

$$\left.\frac{\partial\varphi}{\partial y}\right|_{y=0} = -\left.\frac{2\pi t_B}{\Phi_0}B_z\right|_{y=0} \qquad \left.\frac{\partial\varphi}{\partial y}\right|_{y=W} = -\left.\frac{2\pi t_B}{\Phi_0}B_z\right|_{y=W}$$

Problem: $\boldsymbol{B} = \boldsymbol{B}^{\mathrm{ex(ternal)}} + \boldsymbol{B}^{\mathrm{el(ectrode)}}$

→ $\boldsymbol{B}^{\mathrm{el}}$ not negligible

→ Junction geometries are complicated

→ Current distribution in electrodes depends on current distribution in JJ itself

→ Boundary conditions depend on solution

→ Numerical iteration method required

J. Mannhart, J. Bosch, R. Gross, R. P. Huebener
Phys. Lett. A 121, 241 (1987)

Three basic types of junction geometries

→ Overlap junction

→ In-line junction

→ Grain boundary junctions

2.3.3 Junction Types and Boundary Conditions

Overlap junction

→ Overlap of width W

→ Junction of length L extends in z-direction

→ Perpendicular to current flow

→ $B^{\mathrm{el}} \parallel z$ → $\perp$ to the short side

→ $\Phi^{\mathrm{el}} = B^{\mathrm{el}} \times W \times t_B$ negligibly small

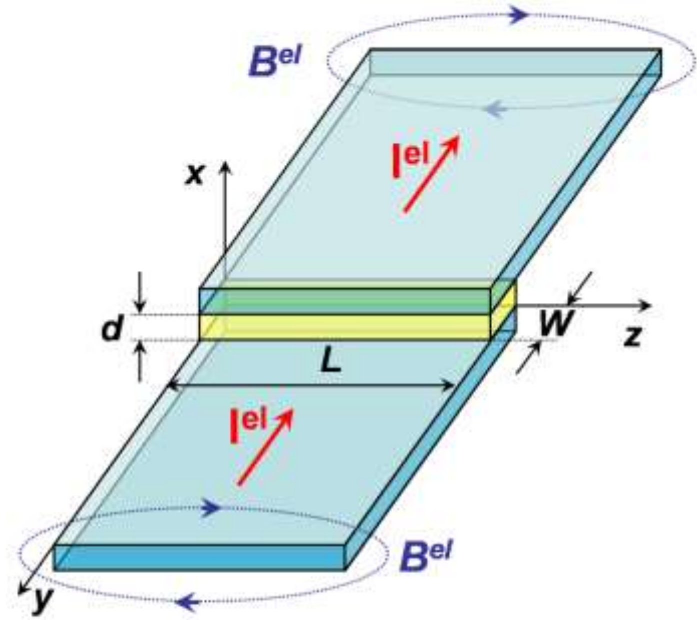

Inline junction

→ Overlap of length L

→ Junction of length L extends in z-direction

→ Parallel to current flow

→ $B^{\mathrm{el}} \perp z$ → $\parallel$ to the short side

→ $\Phi^{\mathrm{el}} = B^{\mathrm{el}} \times L \times t_B$ not negligible

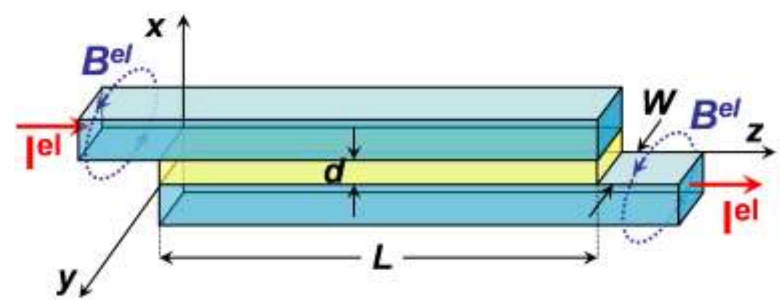

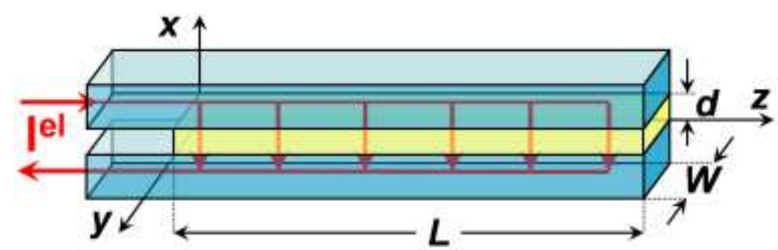

Grain boundary junction

→ Mixture of overlap and inline geometry
→ Junction area is perpendicular to electrode currents
→ Junction area extends in yz-plane
→ Perpendicular to current flow
→ Both y- and z-component of B^{el} are in junction plane
→ B_z^{el} has negligible impact since $W \ll L$
→ $\Phi_z^{\mathrm{el}} = B_z^{\mathrm{el}} W t_B \ll \Phi_y^{\mathrm{el}} = B_y^{\mathrm{el}} L t_B$
→ Finite inline admixture $s = \frac{W}{L} \ll 1$

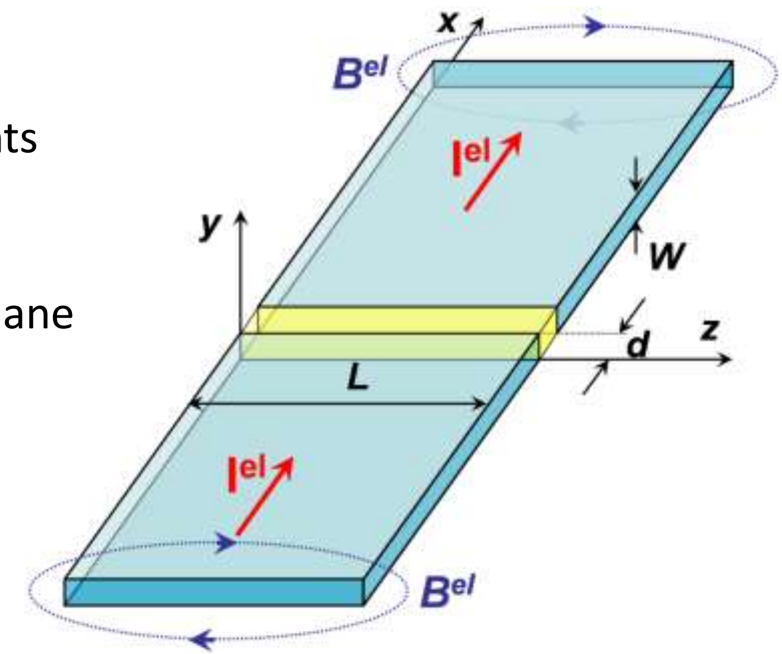

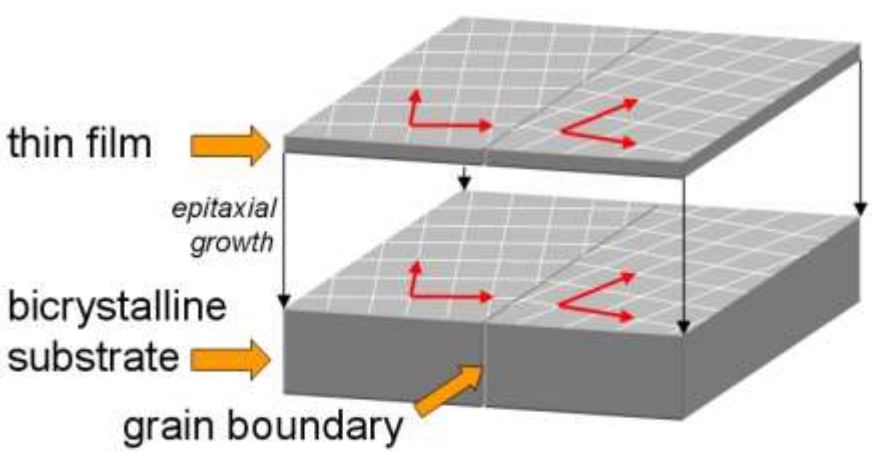

HTS bicrystal grain boundary junction

$I_s^{\mathrm{m}}(B^{\mathrm{ex}})$ for different junction geometries

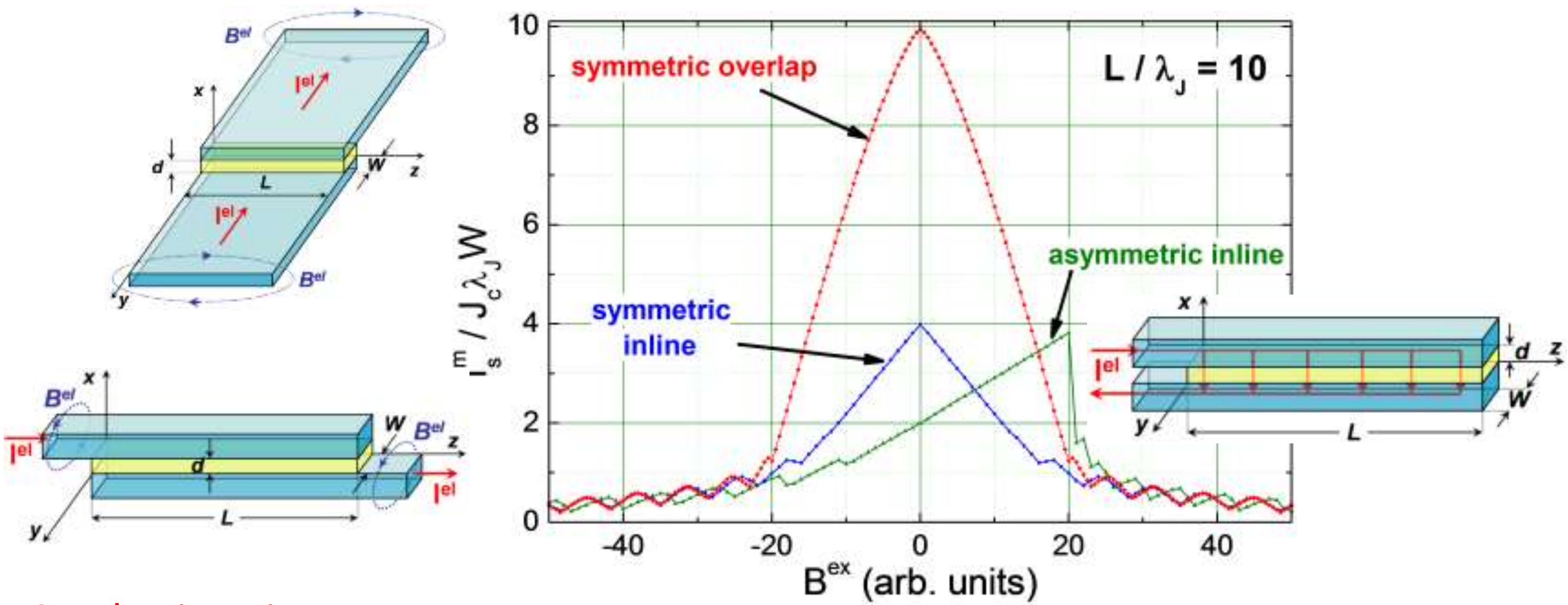

Overlap junction

→ Highest $I_s^{\mathrm{m}} \propto$ junction area $A_i = L \times W$ at zero field

Inline junction

→ I_s^{m} saturates at $4J_c W \lambda_{\mathrm{J}}$ (Meißner screening, current flow at edges)

Asymmetric inline junction

→ Fields generated in bottom and top electrode point in the same direction

→ Adds to/subtracts from external field

→ Increase or decrease of I_s^{m} with field

2.3.4 The Pendulum analog

SSGE equivalent to equation of motion of pendulum (neglecting electrode currents)

→ $z \to t, \varphi \to \theta, \frac{1}{\lambda_J^2} \to \omega_0^2 = \frac{g}{\ell}$

$$\frac{\partial \varphi}{\partial z} = \frac{2\pi}{\Phi_0} B_y t_B$$

θ Angle of the pendulum measured from the top

ω_0 Natural frequency of the pendulum

Pendulum with very large E_{kin}

→ Gravitational acceleration negligible

→ Corresponds to limit of $\lambda_J \to \infty$

→ $\frac{\partial^2 \varphi}{\partial z^2} = 0$ and $\frac{\partial \varphi}{\partial z} = const.$

→ Sinusoidal variation of $J_s(z)$

Pendulum with less E_{kin}, but still nonzero kinetic energy at top

→ $\theta(t)$ anharmonic

→ Corresponds to nonsinusoidal, periodically reversing $J_s(z)$

→ Each spatial cycle of the oscillating current contains one flux quantum

→ In this case, Josephson vortices are localized entities

2.3.4 The Pendulum analog

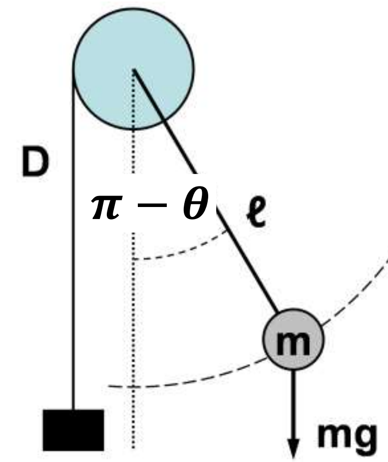

Pedulum with E_{kin} just sufficient to go over the top

→ Meißner limit

→ Start at $-\theta_0$ with $\left(\frac{d\theta}{dt}\right)_0$ at time t corresponding to $-\frac{L}{2}$

→ Pendulum moves very slowly for long time while going over top (interior of junction)

→ Exponential acceleration, recovering initial velocity at θ_0 (at time t corresponding to $+\frac{L}{2}$)

→ Negligible energy at the top

→ Conservation of energy connects θ_0 and $\left(\frac{d\theta}{dt}\right)_0$

$$\left(\frac{2\pi}{\Phi_0}B_y t_B\right)^2 = \left(\frac{d\varphi}{dz}\right)_0^2 = \frac{2}{\lambda_J^2}(1-\cos\varphi_0) \;\Rightarrow \cos\varphi_0 = 1 - \frac{1}{2}\left(\frac{B_y}{\mu_0 J_c \lambda_J}\right)^2$$

→ Small fields → $\varphi_0 = \frac{B_y}{\mu_0 J_c \lambda_J}$ (Taylor expansion of cosine!)

→ Strongest field that can be screened is $B_{\max} = 2\mu_0 J_c \lambda_J$ (for $\varphi_0 = \pi$)

→ (Screening at $B_{\max}$ is only metastable!)

Summary (short junctions)

Josephson penetration depth $\lambda_J \equiv \sqrt{\frac{\Phi_0}{2\pi\mu_0 t_B J_c}}$ (short – long junctions)

Josephson coupling energy $E_J = \frac{\Phi_0 I_c}{2\pi}(1-\cos\varphi) = E_{J0}(1-\cos\varphi)$

nonlinear inductance $L_s = \frac{\Phi_0}{2\pi I_c \cos\varphi} = L_c \frac{1}{\cos\varphi}$ $\quad L_c = \frac{\hbar}{2eI_c}$

washboard potential $E_{\text{pot}}(\varphi) = E_{\text{J}}(\varphi) - \frac{\Phi_0}{2\pi} I\varphi = E_{\text{J0}}\left[1 - \cos\varphi - \frac{I}{I_c}\varphi\right]$

in-plane magnetic field B_y $\quad \frac{\partial\varphi}{\partial z} = \frac{2\pi}{\Phi_0} B_y t_B$

spatial oscillations of the Jospehson current density:

$$\Rightarrow J_s(y,z,t) = J_c(y,z)\sin\left(\frac{2\pi}{\Phi_0} t_B B_y z + \varphi_0\right) = J_c(y,z)\sin(kz+\varphi_0)$$

integral Josephson current → FT of $i_c(z)$:

$$\Rightarrow I_s^m(B_y) = \left| \int_{-\infty}^{\infty} i_c(z) e^{\imath kz} dz \right| \qquad i_c(z) = \int_{-W/2}^{W/2} J_c(y,z) dy$$

Summary (long junctions)

SSGE: spatial distribution of gauge invariant phase difference:

$$\frac{\partial^2\varphi(y,z)}{\partial y^2} + \frac{\partial^2\varphi(y,z)}{\partial z^2} = \frac{2\pi\mu_0\, t_B J_c}{\Phi_0}\sin\varphi(y,z) = \frac{1}{\lambda_J^2}\sin\varphi(y,z)$$

self-consistent solution: boundary conditions depend on flux density at edges

3 basic types: inline, overlap and grain boundary junctions

particular solution of SSGE: Josephson vortex

$$\varphi(z) = \pm 4\arctan\left\{\exp\left(\frac{z-z_0}{\lambda_J}\right)\right\} + 2\pi n$$

Insight into the solutions for $\varphi(z)$ can be found via the pendulum analog

SSGE equivalent to equation of motion of pendulum

$z \to t,\ \varphi \to \theta,\ \frac{1}{\lambda_J^2} \to \omega_0^2 = \frac{g}{\ell}$